The Canadian Mineralogist
Vol. 42, pp. 1629-1649 (2004)

PREDICTION OF CRYSTAL MORPHOLOGY OF COMPLEX URANYL-SHEET MINERALS. I. THEORY

MICHAEL SCHINDLER[§] AND ANDREAS MUTTER

Institut für Mineralogie, Universität Münster, Corrensstr. 24, D-48149 Münster, Germany

FRANK C. HAWTHORNE

Department of Geological Sciences, University of Manitoba, Winnipeg, Manitoba R3T 2N2, Canada

ANDREW PUTNIS

Institut für Mineralogie, Universität Münster, Corrensstr. 24, D-48149 Münster, Germany

ABSTRACT

Edges on the basal face of uranyl-sheet minerals control dissolution and crystal-growth processes because of their higher interaction with the aqueous solution than the less reactive basal face. A basal face is parallel to the structural unit of a uranyl-sheet mineral and dominates its crystal morphology. Edges terminate a structural unit and define the morphology of the prominent basal face. Edges are parallel to linear periodic chains of polyhedra in the structural unit, at which anion terminations interact with a coexisting aqueous solution through acid–base reactions and acceptance of weaker bonds from cationic aqueous species. The bond-valence deficiency of an anion at an anion termination correlates with the intrinsic acidity constant, *pKa*, and the free energy, ΔG_{at}, of the corresponding protonation-type reaction. The degree of interaction of an edge with the coexisting aqueous solution can be described by the bond-valence deficiency per unit length of the anion terminations on the corresponding chain of polyhedra, *i.e.*, an edge at which each site is activated by interaction with aqueous species. The type and number of activated sites on an edge correlate with the bond-valence deficiency of the corresponding chain of polyhedra. Growth and dissolution at an edge are promoted by interaction between activated sites and aqueous solution. The interaction has its minimum at the point of zero-charge (pH_{pzc}) of the edge and at saturation with respect to the mineral, and increases with the difference between pH and pH_{pzc}, and with the degree of saturation. Edges containing a small number of activated sites are stable, grow and dissolve slowly, and invariably occur on the final morphology of the basal face. Edges containing an average number of activated sites are less stable, grow and dissolve faster, and will occur on the final morphology only if crystal growth occurs in solutions with a pH close to pH_{pzc}, and close to saturation with respect to the mineral. Edges with the highest number of activated sites have the lowest stability and may never occur on the final morphology. Interaction of an edge with the aqueous solution depends also on the shift between the layers and the arrangement of the interstitial complexes between the layers.

Keywords: uranyl minerals, morphology, surface structure, crystal growth, dissolution, bond valence.

SOMMAIRE

La bordure de la face parallèle à la base du feuillet des minéraux à uranyle régit la dissolution et les processus de croissance cristalline à cause de sa plus grande interaction avec la solution aqueuse que la face elle-même, moins réactive. Une telle face est parallèle aux unités structurales des feuillets contenant les groupes d'uranyle, et elle est déterminante du point de vue morphologique. Les bordures représentent la terminaison des unités structurales, et définissent la morphologie de la face de base, proéminente. Ces bordures sont parallèles aux chaînes linéaires périodiques de polyèdres de l'unité structurale, là où il y a interaction des terminaisons d'anions avec la solution aqueuse coexistante grâce à des réactions acide–base, et où des liaisons plus faibles provenant d'espèces aqueuses cationiques sont acceptées. Le déficit en valences de liaison d'un anion à la terminaison d'une chaîne d'anions dépend de la constante intrinsèque de l'acidité, *pKa*, et de l'énergie libre, ΔG_{at}, de la réaction correspondante de protonation. On peut décrire le degré d'interaction d'une bordure avec la solution aqueuse coexistante en évaluant le déficit en valences de liaison par unité de longueur des terminaisons des anions dans la chaîne de polyèdres correspondante, c'est-à-dire, une bordure à laquelle chaque site est rendu actif par interaction avec des espèces aqueuses. Le type et le nombre de sites ainsi

§ *Current address*: Department of Geological Sciences, University of Manitoba, Winnipeg, Manitoba R3T 2N2, Canada.
E-mail address: mschindl@lakeheadu.ca

activés à la bordure montre une corrélation avec le déficit en valences de liaison de la chaîne de polyèdres correspondante. La croissance et la dissolution à une telle bordure est accélérée par interactions entre sites activés et la solution aqueuse. L'interaction atteint son minimum au point de charge zéro (pH_{pzc}) de la bordure, et à saturation par rapport au minéral, et augmente avec la différence entre pH et pH_{pzc}, et avec le degré de sursaturation. Les bordures contenant un faible nombre de tels sites activés sont stables, croissent et se dissoudent lentement, et sont normalement développées dans l'expression morphologique finale de la face de base. Les bordures contenant un nombre moyen de tels sites activés sont moins stables, croissent et se dissoudent plus rapidement, et seront présentes dans l'expression morphologique finale de la face de base seulement si la croissance cristalline se déroule dans des solutions ayant un pH voisin de pH_{pzc}, et à des conditions voisines de la saturation par rapport au minéral. Les bordures ayant le nombre de sites activés le plus élevé auront une stabilité moindre, et pourraient bien ne pas être présentes dans l'expression morphologique finale. L'interaction d'une bordure avec la solution aqueuse dépend aussi du degré de déplacement entre les feuillets et de l'arrangement des complexes interstitiels entre les feuillets.

(Traduit par la Rédaction)

Mots-clés: minéraux d'uranyle, morphologie, structure de la surface, croissance cristalline, dissolution, valences de liaison.

Introduction

The morphology of a crystal, the geometry of an etch pit and the characteristics of two-dimensional growth islands on a crystal surface are presumably related to the structural arrangement of atoms in the crystal. This connection was explored by Hartman & Perdok (1955a, b, c), who developed the PBC (Periodic Bond-Chain) theory. The basic idea is as follows: when an atom or complex attaches to a growing surface of a crystal during crystallization, the probability of subsequent detachment is inversely proportional to the number of strong bonds between the atom or complex and the crystal surface. Thus, in PBC theory, the focus is on uninterrupted chains of strong bonds between building units, called PBCs, in which the strong bonds belong to the primary coordination of an atom or molecule. PBC chains that contain only strong bonds between atoms or molecules define the direction of major growth of a crystal, and PBC chains containing weaker bonds between atoms define directions of minor growth. PBC theory distinguishes three different types of faces: F (or flat) faces with two or more types of PBCs (periodic bond-chains) parallel to the face; S (or stepped) faces with one type of PBC parallel to the face, and K (or kinked) faces with no PBCs parallel to the face. In PBC theory, the morphology of a crystal is controlled by the occurrence of F faces. The prediction of morphology from the crystal structure involves (1) determination of PBCs, and (2) classification of (*hkl*) layers as F, S or K faces.

An alternative approach to the morphology of a crystal is to use molecular modeling (with either empirical or quantum-mechanical models) to calculate surface energies or step energies. The surface energy is the difference in energy between the bulk structure and the surface structure; thus, the lower the surface energy, the more stable the face. The step energy is the difference in energy between the surface and the corresponding step; thus, the lower the step energy, the more stable the step. Using such calculations, one can categorize different faces or steps, and calculate the energy of any face or step that might occur in a crystallization or dissolution process. These calculations work well as long as accurate interaction potentials are available for the constituent species. This is not usually the case for complex hydroxy-hydrated oxysalt minerals, which contain unusual coordination geometries and both (OH) and (H_2O) groups, *e.g.*, althupite, Al Th [(UO_2) {$(UO_2)_3$ $(PO_4)_2$ (OH) O}$_2$] $(OH)_3$ $(H_2O)_{15}$. This situation is unsatisfactory, as hydroxy-hydrated oxysalts constitute the bulk of the mineral kingdom and are by far the most important phases from an environmental perspective. Moreover, we know far less about the factors that control their atomic arrangements, chemical compositions, morphology, dissolution and stabilities than for the (usually) more simple rock-forming minerals. Here, we develop a more mechanistic approach to crystallization, dissolution and crystal morphology, and apply it to uranyl-sheet minerals. In addition, we measure the *pKa* value for dehydrated schoepite in order to compare it with the *pKa* value calculated with the MUSIC model of multisite complexation.

Surface Features on Basal Faces

Chemical reactions on the surfaces of uranyl-sheet minerals are an important issue, as they result in the release of $(UO_2)^{2+}$ to natural waters. Therefore, a detailed atomic-scale understanding of the surface chemistry of uranyl-sheet minerals is desirable. Uranyl-sheet minerals contain layers of polymerized uranyl-polyhedra with uranium in [6], [7] and [8]-coordination as tetragonal, pentagonal and hexagonal bipyramids, respectively. In these polyhedra, strong U–O uranyl bonds are not involved in linkage between uranyl polyhedra; they extend orthogonal to the sheet, whereas weaker equatorial U–φ bonds [φ = O^{2-}, $(OH)^-$, (H_2O)] link the polyhedra in the plane of the sheet (Fig. 1).

Periodic Bond-Chain theory (Hartman & Perdok 1955a, b, c) defines the basal face parallel to the sheets of uranyl polyhedra as an F face because the sheet contains more than one periodic bond-chain. If one considers polyhedra instead of bonds, a linear periodic bond-chain is part of a linear periodic chain of polyhe-

dra, which we will designate as a *polyhedron chain* or *chain*. A polyhedron chain that terminates a sheet contains ligands that bond either to U^{6+} cations or to U^{6+} cations *and* to species in the adjacent gas phase or aqueous solution. Any anion on a terminating chain, and the cations to which it is bonded, form a *termination*. The linearity of the chain of polyhedra requires that polyhedra should have a small number of U–φ terminations. In the case of uranyl minerals, we consider only those chains in which each polyhedron has no more than two terminations of the type $U-^{[1]}\varphi$. Figure 1 shows chains of polyhedra parallel to [100], [010], [120], [210] and [110] in the structural unit of schoepite, $[(UO_2)_8O_2(OH)_{12}](H_2O)_{12}$ (Finch *et al.* 1996).

The basal face of a uranyl-sheet mineral is the face parallel to the layers of uranyl polyhedra. Addition of one or more of these uranyl layers can form surface features such as *terraces* and *steps* on the basal face. The termination of one structural unit orthogonal to the basal face is called an *edge*. An array of coplanar edges defines a *step* or a *face* non-coplanar with the basal face. The edge and basal surfaces vary in reactivity owing to differences in the local stereochemistry of their constituent uranyl polyhedra. The reactivity of the basal surface is determined primarily by the reactivity of the apical atoms of oxygen of the uranyl group, $(UO_2)^{2+}$. These oxygen atoms receive an average of 1.6–1.7 valence units (*vu*) from the U–O bond, and hence they cannot be protonated (by H^+), as each O–H bond has an average bond-valence of 0.80 *vu*, and the aggregate incident bond-valence at the uranyl O-atom would be 1.6 + 0.8 = 2.4 *vu*, in conflict with the valence-sum rule (Brown 1981, Hawthorne 1994, 1997). Apical oxygen atoms of the uranyl group are therefore not involved directly in any acid–base reactions at the surface.

Equatorial oxygen atoms in the sheet of polyhedra commonly bond to two or three U^{6+}-atoms (Fig. 1). In contrast to the uranyl bonds, equatorial U–O bond-lengths vary over a larger range, with average bond-valences between 0.2 and 0.8 *vu*. Thus, equatorial O-atoms at basal and edge surfaces can participate in acid–base reactions through protonation and deprotonation. Hence, edge surfaces are much more reactive than basal surfaces because equatorial O-atoms on the edge surface almost always bond to fewer atoms of U^{6+} than O-atoms in the sheet, and hence must satisfy their

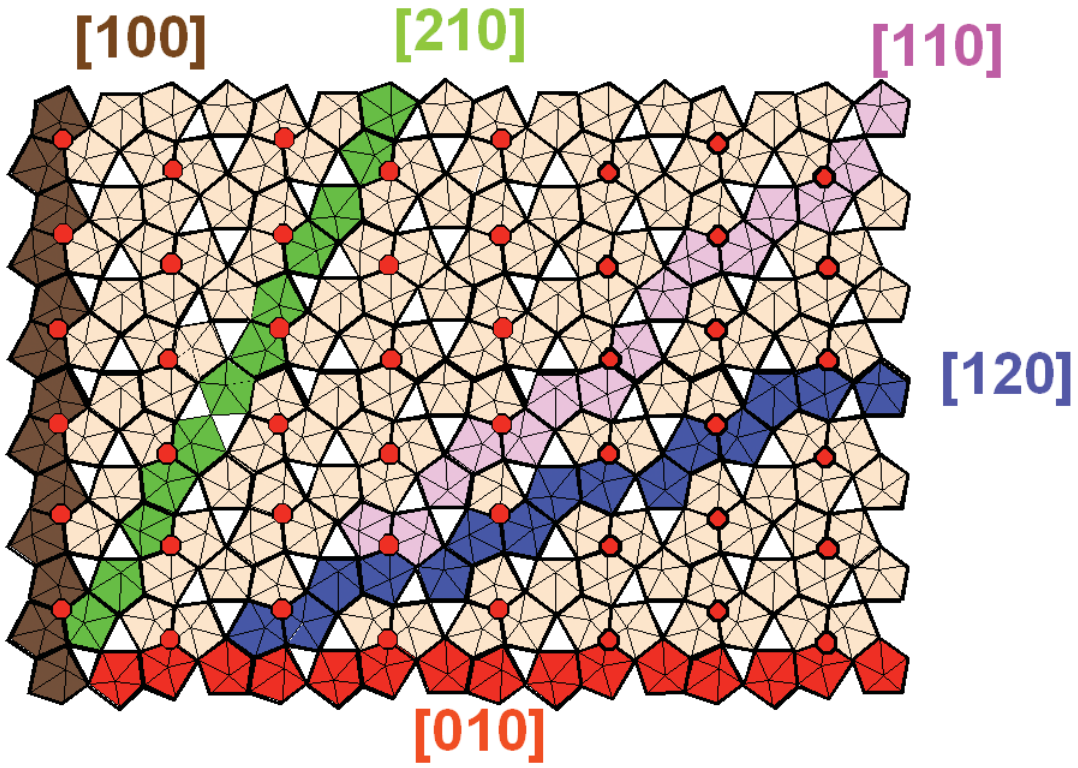

FIG. 1. Polyhedron representation of the uranyl-oxide hydroxy-hydrate sheet in schoepite, $[(UO_2)_8O_2(OH)_{12}](H_2O)_{12}$; chains of polyhedra parallel to [100], [010], [120], [110] and [210] are shown in brown, red, blue, pink and green, respectively; equatorial O^{2-} anions of the uranyl polyhedra are shown as red octagons, equatorial edges are shown as heavy black lines.

individual bond-valence requirements through a higher degree of protonation.

The reactivity of edges is an important factor in the dissolution of sheet minerals; for example, the dissolution of phyllosilicates is controlled by acid–base reactions on the corresponding edges (*e.g.*, Rufe & Hochella 1999). Thus in order to understand dissolution and growth processes for uranyl-sheet minerals, one requires details of the structures of their edges. Inspection of Figure 1 suggests the following question: which periodic bond-chains in uranyl sheets define the morphology of the corresponding F-faces? Application of PBC theory requires categorization of different types of bonds in these bond chains. Bonds between U^{6+} and O^{2-} or $(OH)^{-}$ can have similar strengths in all these chains, and therefore one must consider the distances to the central U^{6+} cations. PBC theory does not consider the type of equatorial ligands in the chain [O^{2-} or $(OH)^{-}$], the shift between the uranyl sheets, the arrangement of interstitial cations, the change in morphology with pH or the degree of supersaturation (see below). Here, we introduce an approach to crystal morphology that considers these issues, using characteristic bond-valence values between U^{6+} and its equatorial ligands. Furthermore, we will show that change in morphology with pH depends on the equilibrium constants of the anion terminations on the surface of uranyl-oxide minerals. For the surface structure of schoepite, $[(UO_2)_8O_2(OH)_{12}](H_2O)_{12}$, we calculate the bond-valence deficiencies for the various types of chains of polyhedra and use the equation of Hiemstra *et al.* (1996) to calculate the corresponding *pKa* values of the acid–base reactions on the anion terminations of the chains. In addition, we measure the *pKa* value of the anion terminations on the basal face of dehydrated schoepite by titration of a fine suspension of synthetic dehydrated schoepite, to compare with our calculated values.

Bond-Valence Theory

Quantitative bond-valence parameters were introduced by Brown & Shannon (1973), and Brown (1981) developed the first ideas on bond-valence theory. Hawthorne (1985, 1990, 1994) applied these ideas to complex oxysalt minerals and developed the idea of the structural unit with a characteristic Lewis basicity. Schindler & Hawthorne (2001a, b, c, 2004) and Schindler *et al.* (2000) extended these ideas and showed how extended bond-valence theory can be used to predict details of mineral composition and stability that are not accessible to other approaches. There has been some application of bond-valence ideas to mineral surfaces (*e.g.*, Barger *et al.* 1997a, b, c, Brown & Parks 2001), but this has focused on adsorption of "foreign" ions rather than on crystallization of the mineral itself.

Bond valence and the valence-sum rule

If interatomic distances are known, bond valences can be calculated from the following equations:

$$s = s_0\,[R / R_0\,]^N,\ s = [R / R_1]^n$$

or

$$s = \exp\,[(R / R_o) / B] \qquad (1)$$

where s is in valence units (*vu*), R is the observed bond-length, and R_0, N, R_1, n and B are constants (characteristic of cation–anion pairs) that are derived by fitting these equations to a large number of well-refined crystal structures such that the sum of the incident bond-valences at any atom be as close as possible to the formal valence of that atom (Brown & Shannon 1973, Brown & Altermatt 1985). In stable (observed) crystal structures, the *valence-sum rule* is obeyed: *the sum of the bond valences at each atom is approximately equal to the magnitude of the atomic valence*.

Characteristic bond-valence

Bond valences around a specific cation in a wide range of crystal structures lie within ~20% of the mean value, which is thus *characteristic* of that particular cation (Brown 1981). The characteristic bond-valences of cations correlate strongly with their *electronegativity*, a measure of the electrophilic strength (electron-accepting capacity) of the cation. The correlation with characteristic bond-valence indicates that the latter is a measure of the *Lewis-acid strength* of the cation (Brown 1981). The Lewis-base strength of an anion is similarly defined as the characteristic valence of the bonds formed by the anion. However, variations in bond valence around anions are much greater than around cations, and it is not useful to designate Lewis basicities for simple anions such as O^{2-}.

If we examine the $(CO_3)^{2-}$ group as an oxyanion, each O^{2-} receives 1.33 *vu* from the central C^{4+} cation and needs an additional 0.67 *vu* from other cations. In calcite, for example, the oxygen atoms of the $(CO_3)^{2-}$ group are [3]-coordinated, and hence need an additional two bonds if we consider the $(CO_3)^{2-}$ group as an oxyanion; the additional bond-valence needed is thus 0.33 *vu* for each of the oxygen atoms of the $(CO_3)^{2-}$ group. If this process is repeated for all (CO_3) groups in minerals, the mean value of the characteristic bond-valence obtained is 0.25 *vu* with only a small dispersion. In this way, we can define the *Lewis basicity* of an oxyanion (Brown 1981).

The valence-matching principle

The definitions of Lewis-acid and Lewis-base strengths lead to a specific criterion for chemical bond-

ing, the *valence-matching principle* (Brown 1981): *The most stable structures will form where the Lewis-acid strength of the cation closely matches the Lewis-base strength of the anion*. As a chemical bond contains two constituents, the properties of the constituents must match for a stable configuration to form.

Binary Structural Representation

One of the problems in dealing with mineral structures is the complexity of the atomic interactions; there are a large number of such interactions, and their spatial characteristics are important. However, we can simplify this problem in the following way: we factor a crystal structure into two components: the *structural unit* (an array of high-bond-valence polyhedra that is usually anionic in character) and the *interstitial complex* [an array of large low-valence cations, simple anions and (H_2O) groups that is usually cationic in character]. If we can calculate aggregate properties such as Lewis basicity and Lewis acidity, we can use the valence-matching principle to examine the interaction of the structural unit and the interstitial complex (Hawthorne 1985, 1986, 1990). Schindler & Hawthorne (2001a) described how to calculate Lewis basicity and Lewis acidity for a structural unit and an interstitial complex.

Interaction of a Surface with an Aqueous Solution: a Bond-Valence Approach

As noted above, the bond-valence sum incident at any cation or anion must be equal to its formal valence. In the bulk structure, the bond valences contributing to such a sum involve simple ions at the vertices of the associated coordination-polyhedra. With regard to a surface, we may identify two distinct situations: (1) the surface of the crystal is adjacent to a vacuum; (2) the surface of the crystal is adjacent to a liquid (or a gas). In the first situation, the ions at the surface of a crystal by definition must have coordinations different from those in the bulk crystal, and these differences will exist over long time-scales. The surface structure responds to these differences by lengthening or shortening specific bonds; such differences in bond lengths (and bond angles) are commonly called the *relaxation* of the surface. As a result of these differences, the pattern of bond valences at and near the surface in a vacuum must differ significantly from that in the bulk crystal, even to the extent that there may be a reorganization of the topology of the chemical bonds at the surface. In the second situation, although the atoms at the surface must have coordinations different from those in the bulk crystal, the bond-valence requirements of these surface atoms are also partly met by neighboring atoms in the coexisting liquid (or gas). Hence surface relaxation will be much less than where the surface is exposed to a vacuum. Indeed, the atoms of the liquid will tend to arrange themselves such that relaxation at the surface of the solid is minimized, and one may well be able to consider local interactions among atoms as the average of what occurs at the surface over a longer time-scale. This discussion suggests that we may be able to use an unrelaxed surface model in which one treats bond valences of near-surface bonds as equal to the bond valences of the analogous bonds in the bulk structure.

Intrinsic acidity constants of anion terminations in oxide minerals

Consider a crystal in equilibrium with an aqueous solution. Depending on the pH of the solution, the surface is partly or fully hydrated, and aqueous species in the solution bond to anions or cations on the surface (chemisorption). The degree of hydration and type of chemisorption depend on the type of anion or cation on the surface and on the conditions in the coexisting solution. The degree of hydration can be predicted with the acidity constants of the different anion-terminations and the pH of the solution. Van Riemsdijk and co-workers (Hiemstra *et al.* 1996) developed a "multisite complexation model" (MUSIC), which can be used to predict anion acidities using a modified form of the following equation:

$$pKa = -A\ (\Sigma s_j + V) \tag{2}$$

where pKa is the intrinsic acidity constant [a constant valid for an uncharged surface (Stumm 1992)], A equals 19.8, V is the valence of the oxygen atom at the surface (–2), and Σs_j is the bond-valence sum at the surface oxygen atom and is defined by

$$\Sigma s_j = \{s_M + ms_H + n(1 - s_H)\} \tag{3}$$

where s_M is the bond valence of the M–O bond, s_H is the bond valence of the H–O bond to the surface oxygen if the base is a hydroxyl group (assumed to be 0.80 *vu*), $(1 - s_H)$ is the valence of weak hydrogen bonds from aqueous species to surface anions, and m and n are the numbers of stronger O–H and weaker O…H bonds, respectively. Hiemstra *et al.* (1996) used fixed M–O bond-valences from unrelaxed bulk-structures to predict intrinsic acidity constants for surface groups. Bickmore *et al.* (2003) used *ab initio* calculations for the average of M–O bond-valences of protonated and deprotonated relaxed surface-structures in 2:1 phyllosilicates; their average bond-valence values for Fe–O, Al–O and Si–O bonds are similar to the corresponding values used by Hiemstra *et al.* (1996).

The key issue in the prediction of appropriate intrinsic acidity-constants is use of the correct *average coordination number of O* on the surface. Here, Hiemstra *et al.* (1996) used an average coordination of oxygen of [3] for the more compact surfaces of gibbsite and goethite, and an average coordination number of [4] for the more open surface of quartz. The resulting intrinsic acid-

ity-constants were used to calculate the point of zero-charge (pH_{pzc}, Stumm 1992) for gibbsite, goethite and quartz, and the results agree with experimental values.

Calculation of intrinsic acidity-constants for different U–O anion-terminations on edges of the basal face of uranyl-sheet minerals

The edges on uranyl sheets contain equatorial anions in a coordination different from that in the bulk structure. For tetragonal, pentagonal and hexagonal bipyramidal coordination, the characteristic equatorial U–φ bond-valences are 0.64, 0.54 and 0.45 *vu*, respectively (Burns 1999). However, individual equatorial $^{[a]}$U–φ bond-lengths vary over a larger range than the corresponding Al–O, Fe–O and Si–O bond-lengths. For example, the $^{[7]}$U–φ bond-lengths in schoepite, $[(UO_2)_8O_2(OH)_{12}](H_2O)_{12}$, vary between 2.2 and 2.7 Å (Finch *et al.* 1996), which correspond to bond valences of 0.73 and 0.27 *vu*, respectively. These high variations in individual bond-valences in uranyl minerals may give rise to a range of intrinsic acidity-constants for one type of anion termination.

The type of anion termination on edges in uranyl minerals is limited by the occurrence of [6]-, [7]- and [8]-coordinated U^{6+}: *e.g.*, [6]- and [8]-coordinated U^{6+} never occur together, and always occur with [7]-coordinated U^{6+}. The type of anion termination can be indicated by the code $^{[a]}$U–φ–*n*$^{[b]}$U, where the φ is an unspecified anion that bonds to one U atom in [*a*] coordination and *n* × U atoms in [*b*] coordination. If we do not consider other oxyanions [*e.g.*, $(VO_4)^{3-}$, $(PO_4)^{3-}$, $(SiO_4)^{4-}$], the following combinations of anion terminations can occur on edges in uranyl-oxide sheet minerals: $^{[8]}$U–φ, $^{[7]}$U–φ, $^{[6]}$U–φ, $^{[8]}$U–φ–$^{[8]}$U, $^{[8]}$U–φ–$^{[7]}$U, $^{[7]}$U–φ–$^{[7]}$U, $^{[7]}$U–φ–$^{[6]}$U, $^{[8]}$U–φ–2$^{[7]}$U, $^{[7]}$U–φ–2$^{[7]}$U and $^{[6]}$U–φ–2$^{[7]}$U. The wide variation in type of anion termination (even for one structure type) makes it difficult to determine an exact pH_{pzc} for a uranyl mineral. However, an exact pH_{pzc} is required to scale the average coordination-number of the oxygen atoms on the edge surface (see above).

An example: calculation of the intrinsic acidity-constants of anion terminations on the (001) face of schoepite

Schoepite, $[(UO_2)_8O_2(OH)_{12}](H_2O)_{12}$, has a prominent (001) basal face that dominates the morphology of its crystals. The corresponding uranyl-sheet contains U^{6+} in [7]-coordination (Finch *et al.* 1996). There are three different types of equatorial anion-terminations on the (001) face: $^{[7]}$U–OH–2$^{[7]}$U, $^{[7]}$U–OH–$^{[7]}$U and $^{[7]}$U–O–2$^{[7]}$U (Fig. 1). In order to calculate the corresponding intrinsic *pKa* values for these terminations, we can use the overall characteristic bond-valence for $^{[7]}$U–φ (0.54 *vu*), the average $^{[7]}$U–φ bond-valence of the equatorial bonds in schoepite (0.47 *vu*), or the average $^{[7]}$U–φ bond-valence for each of the three anion-terminations. Here, we use the average bond-valence of the equatorial bonds (0.47 *vu*) because this value is more appropriate than the characteristic $^{[7]}$U–φ bond-valence, and it simplifies the calculation (relative to the use of individual average bond-valences). In many uranyl-hydroxy-hydrate minerals, the coordination number of equatorial O-atoms in the structural unit is close to [4]; oxygen bonds either to three U and one H, or to two U, one H and accepts one additional hydrogen bond.

The acid–base reactions and the corresponding values of *pKa* (assuming $^{[4]}$O) are as follows:

$$^{[7]}\text{U–O–2}^{[7]}\text{U} + \text{H}^+ \leftrightarrow {}^{[7]}\text{U–OH–2}^{[7]}\text{U}, \quad pKa = 7.7 \qquad [1]$$

$$^{[7]}\text{U–O–}^{[7]}\text{U} + \text{H}^+ \leftrightarrow {}^{[7]}\text{U–OH–}^{[7]}\text{U}, \quad pKa = 13.1 \qquad [2]$$

$$^{[7]}\text{U–OH–}^{[7]}\text{U} + \text{H}^+ \leftrightarrow {}^{[7]}\text{U–OH}_2\text{–}^{[7]}\text{U}, \quad pKa = 1.2 \qquad [3]$$

The intrinsic *pKa* is calculated using the average bond-valence sum at O in the anion termination of the base (*i.e.*, for the termination on the left side of each equation). In reaction [1], the oxygen atom in $^{[7]}$U–O–2$^{[7]}$U receives 3 × 0.47 (from the $^{[7]}$U atoms) + 0.20 (from a hydrogen bond) = 1.61 *vu*. This results in a pKa_1 of –19.8(1.61 – 2) = 7.7. In reaction [2], the oxygen atom in $^{[7]}$U–O–$^{[7]}$U accepts 2 × 0.47 *vu* from $^{[7]}$U, and 2 × 0.20 *vu* from two additional hydrogen bonds; *i.e.*, its bond-valence sum is 1.34 *vu*, which corresponds to a pKa_2 of 13.1. In reaction [3], the oxygen atom in the $^{[7]}$U–OH–$^{[7]}$U termination receives 2 × 0.47 *vu* plus 0.80 *vu* from the O–H bond and 0.20 *vu* from an additional hydrogen bond; its bond-valence sum is 1.94 *vu*, which corresponds to a pKa_3 of 1.2.

In order to compare calculated *pKa* values with observed values, one can determine the *pKa* values of the anion-terminations *via* titration of a fine suspension of schoepite with an NaOH solution. However, schoepite samples with a non-dehydrated surface are difficult to obtain from mineral samples or from synthesis. We decided therefore to use the structurally related phase dehydrated schoepite, which can be easily obtained by hydrothermal synthesis.

Experimental procedure

Dehydrated schoepite, $[(UO_2)O_{0.2}(OH)_{1.6}]$, was synthesized under hydrothermal conditions at 120°C for 3 days with a molar ratio of 1:2.5 uranyl acetate and (H_2O). A fine suspension of 100 mg of dehydrated schoepite in 20 mL 0.1 and 1.0 mol L^{-1} NaCl solutions were titrated with 0.01 mol L^{-1} NaOH. Figure 2 shows the corresponding titration-curves with initial pH-values of 6.2 and 5.9, respectively. [Note that titration of the fine suspension of schoepite with a 0.01 mol L^{-1} HCl

solution produced an immediate drop in pH to 3–3.5.] The shift in the initial pH-values with change in concentration of the NaCl solution indicates adsorption of Na cations at specific sites on the (001) face (Stumm 1992). This adsorption results in an overall positive charge of the surface, which must be balanced by deprotonation of the U–OH–2U terminations. In this way, the (001) face of dehydrated schoepite functions as a weak acid, which explains the slightly acidic pH at the beginning of the titration. Because an NaCl solution is required to maintain a constant ionic medium, we modeled a curve for a titration in a 0.0 mol L^{-1} NaCl solution. The initial pH of the dehydrated schoepite solution in the modeled curve is around 6.5, and the *pKa* value is around 7.0 ± 0.2 (Fig. 2). This *pKa* value corresponds to the acid–base reaction U–(OH)–2U ↔ U–O–2U on the (001) face of dehydrated schoepite. [Note that in the anion-termination U–(OH)–2U of dehydrated schoepite, U occurs in [7]- and [8]-coordination. The [8]-coordination of U in dehydrated schoepite results from dehydration of schoepite and structural changes inside the uranyl sheet.] At the beginning and at the end of the titration, the (001) face of dehydrated schoepite most likely had the compositions $[(UO_2)O_{0.2+x}(OH)_{1.6-2x}]^{2x+}$ and $[(UO_2)O_2]^{2-}$, respectively.

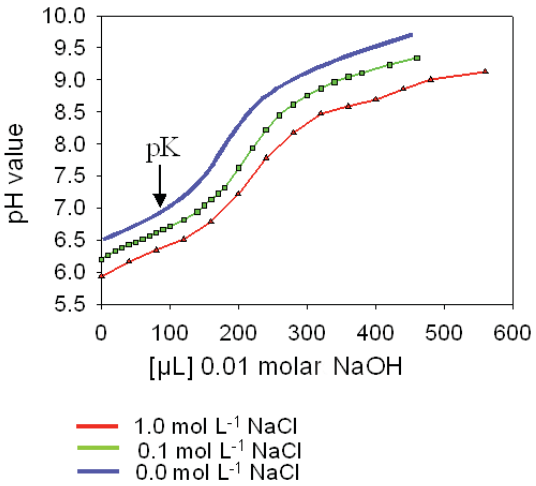

FIG. 2. Titration curves with added 0.01 mol L^{-1} NaOH *versus* pH for a fine suspension of 100 mg of dehydrated schoepite in 20 mL 0.1 mol L^{-1} (green) and 1 mol L^{-1} (red) NaCl solutions. A modeled titration-curve in a hypothetical 0.0 mol L^{-1} NaCl solution is indicated in blue (see text for details).

The calculations of the *pKa* value of schoepite and the experimentally determined *pKa* value of dehydrated schoepite are reasonably close, and suggest that the average coordination-number of [4] is an appropriate value in the case of the uranyl-oxide minerals schoepite and dehydrated schoepite. For example, if one uses an average coordination-number of [3], the intrinsic *pKa* value of the acid–base reaction $^{[7]}$U–O–2$^{[7]}$U + H^+ ↔ $^{[7]}$U–OH–2$^{[7]}$U would be 11.7, significantly different from the observed value of 7.0 ± 0.2.

The parameter 19.8 (equation 2) of the MUSIC model was fitted on the basis of experimental results on simple oxide minerals such as hematite, rutile and quartz. Hence, equation 2 in this form is not necessarily applicable to all uranyl oxide minerals, and needs to be measured in the future on uranyl oxide minerals. However, we will use this equation here in order to show how the intrinsic acidity constant is related to two other parameters that express the strength of a base and an acid: Lewis basicity and Lewis acidity. For this purpose, we calculated intrinsic acidity-constants for all kinds of anion terminations using the above-listed average $^{[n]}$U–φ bond-valences in uranyl polyhedra (Table 1).

TABLE 1. INTRINSIC ACIDITY CONSTANTS, LEWIS ACIDITIES AND LEWIS BASICITIES OF EQUATORIAL ANIONS TERMINATING EDGES ON URANYL-SHEET MINERALS

Code	Acids and bases of the anion-termination	pKa_1, pKa_2, pKa_3	Lewis acidity / Lewis basicity [*vu*]
$^{[8]}$U–φ,	$^{[8]}$U–OH_3 ↔ $^{[8]}$U–OH_2 ↔ $^{[8]}$U–OH ↔ $^{[8]}$U–O	–5, 6.9, 18.8	0.225 / 0.375, 0.52
$^{[7]}$U–φ	$^{[7]}$U–OH_3 ↔ $^{[7]}$U–OH_2 ↔ $^{[7]}$U–OH ↔ $^{[7]}$U–O	–6.7, 5.1, 17	0.27 / 0.33, 0.49
$^{[6]}$U–φ	$^{[6]}$U–OH_3 ↔ $^{[6]}$U–OH_2 ↔ $^{[6]}$U–OH ↔ $^{[6]}$U–O	–8.7, 3.1, 15	0.32 / 0.27, 0.45
$^{[8]}$U–φ–$^{[8]}$U	$^{[8]}$U–OH_2–$^{[8]}$U ↔ $^{[8]}$U–OH–$^{[8]}$U ↔ $^{[8]}$U–O–$^{[8]}$U	2, 13.8	0.30, 0.55
$^{[8]}$U–φ–$^{[7]}$U	$^{[8]}$U–OH_2–$^{[7]}$U ↔ $^{[8]}$U–OH–$^{[7]}$U ↔ $^{[8]}$U–O–$^{[7]}$U	0.2, 12	0.21, 0.51
$^{[7]}$U–φ–$^{[7]}$U	$^{[7]}$U–OH_2–$^{[7]}$U ↔ $^{[7]}$U–OH–$^{[7]}$U ↔ $^{[7]}$U–O–$^{[7]}$U	–1.6, 10.3	0.12, 0.46
$^{[7]}$U–φ–$^{[6]}$U	$^{[7]}$U–OH_2–$^{[6]}$U ↔ $^{[7]}$U–OH–$^{[6]}$U ↔ $^{[7]}$U–O–$^{[6]}$U	–3.5, 8.3	0.02, 0.41
$^{[8]}$U–φ–2$^{[7]}$U	$^{[8]}$U–OH–2$^{[7]}$U ↔ $^{[8]}$U–O –2$^{[7]}$U	5.3	0.47
$^{[7]}$U–φ–2$^{[7]}$U	$^{[7]}$U–OH –2$^{[7]}$U ↔ $^{[7]}$U–O –2$^{[7]}$U	3.5	0.38
$^{[6]}$U–φ–2$^{[7]}$U	$^{[6]}$U–OH –2$^{[7]}$U ↔ $^{[6]}$U–O –2$^{[7]}$U	2.5	0.28

Lewis basicity of anion terminations

The intrinsic acidity-constant *pKa* is a measure of the strength of the acid in an acid–base equation: the higher the *pKa*, the weaker its acid strength or the stronger the base strength of the corresponding base. Using the acid–base definition of Lewis (1916), *pKa* expresses the ability of the base (Lewis base) to donate electrons to the acid (Lewis acid).

Hawthorne (1997) and Schindler & Hawthorne (2001a) defined the Lewis-base strength of a complex structural unit as the bond valence required by the (negatively charged) structural unit divided by the number of (weak) bonds accepted by the structural unit from the interstitial complex. Using this definition, we may calculate the Lewis-base strength (or Lewis-acid strength) of an anion termination by assuming again an average O-coordination number of [4]. For example, the Lewis-base strength of the anion-termination $^{[7]}$U–OH is the required bond-valence [(2 – (0.54 + 0.80) = 0.66 *vu*] divided by the number of bonds accepted (two): 0.66 / 2 = 0.33 *vu*. For the anion termination $^{[a]}$U–OH_2, it is more useful to calculate its Lewis acidity because the constituent O-atom has an incident bond-valence sum greater than or equal to 2 *vu*. The Lewis acidity of the $^{[a]}$U–OH_2 group is the characteristic bond-valence of each constituent hydrogen bond. Hence, the (H_2O) group transforms the bond-valence (*v vu*) of the $^{[a]}$U–O bond into two weaker hydrogen bonds of bond-valence *v* /2 (Hawthorne 1992, 1994, 1997, Schindler & Hawthorne 2001a). For example, the Lewis acidity of the termination $^{[7]}$U–OH_2 is 0.54 / 2 = 0.27 *vu*. The Lewis acidities and Lewis basicities of all anion terminations are listed in Table 1.

Lewis basicity and acidity constants

Let us consider the anion terminations $^{[7]}$U–OH and $^{[7]}$U–O in the acid–base reactions [2] and [3]. The corresponding pKa_2 and pKa_3 values express the ability of the bases $^{[7]}$U–OH and $^{[7]}$U–O to donate electrons to the acid H^+. The Lewis basicities (0.33 and 0.49 *vu*) correspond to the pKa_2 and pKa_3 values of 5.1 and 17, respectively. For the anion termination $^{[a]}$U–OH_2, with [*a*] = [8], [7] and [6], we assign a negative Lewis acidity and correlate it with the corresponding *pKa* value. The anion terminations listed above can be subdivided into five groups: $^{[a]}$U–OH_2, $^{[a]}$U–OH, $^{[a]}$U–O, $^{[a]}$U–OH–2$^{[b]}$U and $^{[a]}$U–O–2$^{[b]}$U. For each group, there is a linear correlation between the Lewis basicity (acidity) and the corresponding *pKa* value (Fig. 3). This correlation can be understood if we compare the corresponding equations for the acidity constant and the Lewis basicity:

$$pKa = 19.8\ [\Delta s - 0.20(4 - a(\text{U–O}) - b(\text{O–H}))] \quad (4)$$

$$(LB) = \Delta s\ /\ [4 - a(\text{U–O}) - b(\text{O–H})] \quad (5)$$

where Δs is the bond-valence deficiency of the O-atom at the anion termination without considering any accepted hydrogen bonds; 0.20 [4 – *a*(U–O) – *b*(O–H)] is the bond-valence contribution of weak hydrogen bonds, where *a* and *b* are the numbers of U–O and O–H bonds, respectively; (*LB*) is the Lewis basicity. Writing [4 –

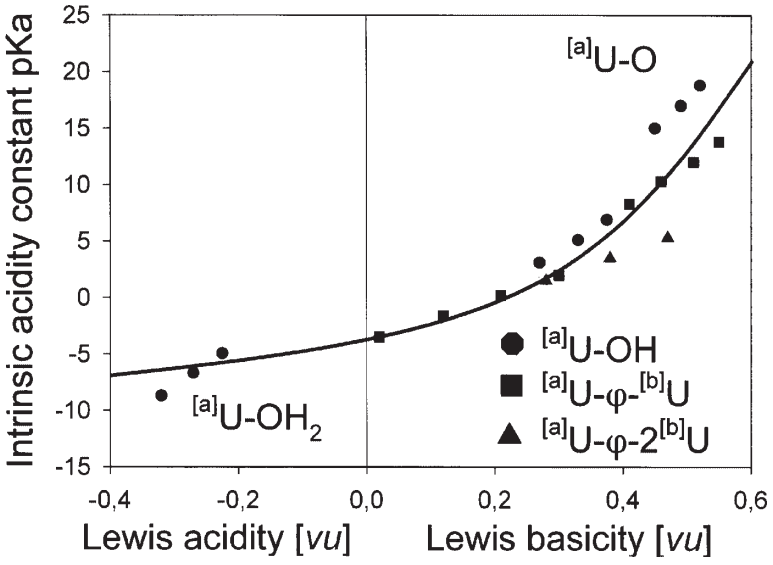

FIG. 3. Lewis basicity *versus* intrinsic acidity constant, *pKa*, of anion terminations on the edges of uranyl sheets (see text).

a(U–O) – b(O–H)] as x and solving for pKa gives the following relation:

$$pKa = 19.8\ (\Delta s.x - 0.2\ x) \quad (6).$$

The parameter x is constant for one group of anion terminations, but varies from group to group (*e.g.*, from 1 in $^{[a]}$U–OH_2 to 3 in $^{[a]}$U–O with a = 6, 7, 8). The correlation between Lewis basicity and pKa for all five groups of anion terminations is shown by the curved line in Figure 2.

Bond-valence deficiency at an anion termination

Calculation of the intrinsic acidity-constant and the Lewis basicity of an anion termination requires knowing the bond-valence deficiency at an oxygen atom [equations (3) and (4)]. The average coordination-number of the oxygen atom at an anion termination scales the absolute values of the intrinsic acidity-constant and the Lewis basicity. The bond-valence deficiency at an oxygen atom is independent of the coordination number of the oxygen, and is a better parameter to characterize the basicity of an anion termination. The bond-valence deficiency at an oxygen atom can be related to the free energy of the acid–base reactions [1], [2] or [3] as follows (Faure 1998):

$$\Delta_R G_{AT} = -2.303\ RT\ pKa \quad (7)$$

where $\Delta_R G_{AT}$ is the free energy of the acid–base reaction at one anion-termination. Combination of equations (3) and (7) results in

$$\Delta_R G_{AT} = -2.303\ RT\ 19.8\ (\Delta s - 0.20\ x) \quad (8).$$

Equations (3), (4) and (7) indicate that the higher the bond-valence deficiency at an oxygen atom, the stronger the basicity of the anion termination, the stronger its affinity to hydrogen bonds or O–H bonds, and the more negative the free energy $\Delta_R G_{AT}$ of the corresponding acid–base reaction.

Bond-valence deficiency, pKa, and free energy of a chain of polyhedra

The bond-valence deficiency of an edge may be defined as the sum of bond-valence deficiencies on anion terminations, normalized to its translation length. A chain of polyhedra in the sheet ideally represents an edge on an F face (Fig. 1). Each type of chain contains different types of anion terminations, and each type of anion termination corresponds to a specific pKa, Lewis basicity, and $\Delta_R G_{AT}$ value of a corresponding acid–base reaction. Let us consider a chain of polyhedra of translation a, with $b \times {}^{[7]}$U–O and $c \times {}^{[7]}$U–O–$^{[7]}$U terminations. The pKa value of an acid–base reaction involving this chain of polyhedra is designated ΔpK_{PC}, and depends on the numbers and types of different anion-terminations. The pKa value of an acid–base reaction involving a chain of polyhedra may be written as $\Sigma\Delta pK_{PC}$, and may be defined as the sum of the pKa values of acid–base reactions at the corresponding anion-terminations per Å.

$$\Sigma\Delta pK_{PC} = [b \times pKa\ (^{[7]}\text{U–O}) + c \times pKa\ (^{[7]}\text{U–O–}^{[7]}\text{U})] / a \quad (9).$$

Equation (9) can be rewritten as

$$\Sigma\Delta pK_{PC} = [b \times \Delta s\ (^{[7]}\text{U–O}) + a \times \Delta s\ (^{[7]}\text{U–O–}^{[7]}\text{U})] / a \quad (10)$$

The term $[b \times \Delta s\ (^{[7]}\text{U–O}) + a \times \Delta s\ (^{[7]}\text{U–O–}^{[7]}\text{U})] / a$ is the O-atom bond-valence deficiency per Å for a chain of polyhedra. It correlates with the average value of pKa and the free energy of acid–base reactions along a chain of polyhedra, and indicates the affinity of the constituent O-atoms for hydrogen bonds or O–H bonds. The bond-valence deficiency per Å can be calculated from crystal-structure data.

Dissolution rate and bond-valence deficiency

Sunagawa (1987) compared different crystal-growth parameters such as growth temperature, solute–solvent interaction, and roughness factor, α, with the corresponding medium of crystal growth, *e.g.*, melt, high-temperature solution, low-temperature solutions, chemical vapor-deposition and physical vapor-deposition. He showed that in low-temperature solutions, the solute–solvent interaction is the most important factor in controlling crystal growth and dissolution rates on surfaces and edges.

Uranyl-sheet minerals crystallize from low-temperature solutions, and the solute–solvent interaction at the edges of the basal faces should be the primary determinant of their stability. The solute–solvent interaction can be described *via* surface-controlled dissolution (Stumm 1992), which gives an understanding of how the dissolution kinetics of surfaces are controlled by protonation or by the presence of inner-sphere complexes. Protonation tends to increase dissolution rate because it leads to weaker bonds proximal to surface cations, and thus facilitates detachment of a surface group into solution. Surface-controlled dissolution is based on the idea that (1) attachment of reactants (H^+, OH^- or ligands) to surface atoms or groups of atoms is rapid, and (2) subsequent detachment of metal species from the surface into solution is slow (and thus rate-limiting). In the first sequence, the dissolution reaction is initiated by bonding to H^+, $(OH)^-$ and ligands that weaken and tend to break *M*–O–*M* bonds at the surface. This is schematically indicated in Figure 4 as a model of dissolution and growth of schoepite *via* detachment and attachment of clusters. The structure of a schoepite sheet is built from clusters

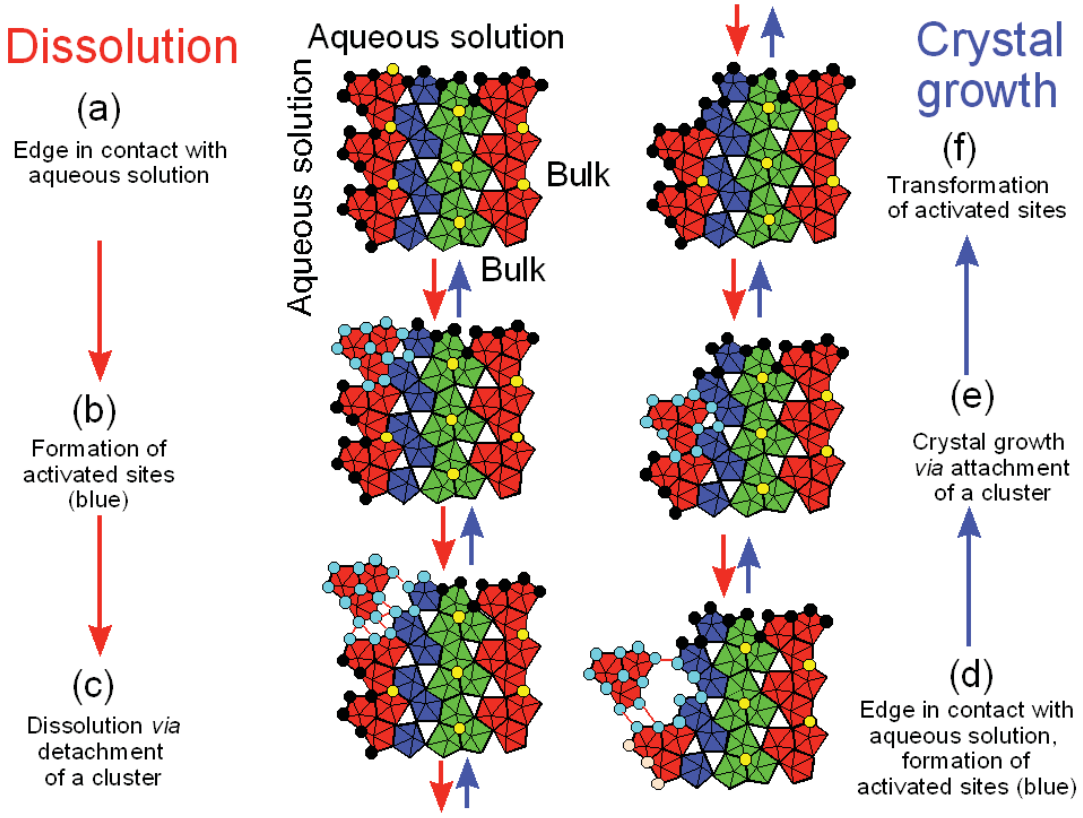

FIG. 4. (a) Schematic sketch of dissolution and growth processes at an edge of a sheet of schoepite. The sequence of dissolution is indicated with red arrows, and the sequence of crystal growth, by blue arrows. The sheet is built of clusters of three (red and green) and two (blue) pentagonal bipyramids that are structurally identical to the principal aqueous species $[(UO_2)_3(OH)_5(H_2O)_5]^+$ and $[(UO_2)_2(OH)_2(H_2O)_6]^{2+}$ in weak acidic solutions (*e.g.*, Moll *et al.* 2000); O^{2-} ligands in the sheet are indicated as yellow circles, and ligands that have interacted with the aqueous solutions are indicated in light blue; (a), (f): activated sites occur only at anion terminations, and activated sites in the layer are transformed to normal sites; (b), (e): formation of activated sites during the dissolution process *via* detachment of a cluster; ligands adjacent to potential detached clusters interact with the solution and are highlighted as light blue octagons; attachment of a cluster at a kink site occurs *via* release of one (H_2O) per common ligand between cluster and kink site; (c), (d): breaking (formation) of the U–φ–U bonds and detachment (or approach) of a cluster from (to) an activated kink-site on a layer of schoepite. Non-activated sites in contact with aqueous solution are indicated as black circles. Possible hydrogen bonds between uranyl clusters in solution and polyhedra at the kink sites are shown as solid pale-brown lines.

of three and two pentagonal bipyramids, which are structurally identical to the aqueous species $[(UO_2)_3(OH)_5(H_2O)_5]^+$ and $[(UO_2)_2(OH)_2(H_2O)_6]^{2+}$ (*e.g.*, Moll *et al.* 2000). These clusters involve edge-sharing pentagonal bipyramids, and link through common edges and corners (Fig. 4). Ligands on terminations interact with the aqueous solution *via* hydrogen bonding or acid–base reactions (Fig. 4a).

If dissolution occurs *via* detachment of clusters, the breaking of U–φ–U bonds occurs mainly at the linking O-atoms. This requires weakening of a number of U–φ bonds in the clusters through interaction between the ligands and the adjacent aqueous solution (Fig. 4b). As this weakening begins, the environment of a detaching cluster may be called an *activated site.* At an activated site, the interaction between aqueous solution and ligands provides the necessary weakening of the corresponding U–φ bonds, which finally break at the detachment of a cluster or a polyhedron (Fig. 4c). Thus an activated site involved in dissolution may be defined as follows: *An activated site involves the terminations around a polyhedron or a cluster of polyhedra where protonation or strong bonds between ligands and aqueous species results in weakening of U–φ bonds.*

If crystal growth occurs *via* attachment of clusters, the activated sites on the cluster and on the kink site of

the surface promote the attachment progress. Attachment produces one additional (H_2O) or (OH) group per common corner between cluster and kink site (Figs. 4d, e). Thus, an activated site involved in crystal growth may be defined as follows: *An activated site involves the terminations on a polyhedron or group of polyhedra where there are strong hydrogen bonds to a polyhedron or cluster of polyhedra in solution.*

The remaining common corners between cluster and former kink-site remain activated until the corresponding ligands do not require any additional bond-valence from bonds to aqueous species (Fig. 4f). Bonds between activated sites and aqueous species promote dissolution or crystal growth at an edge.

Bond-valence deficiency, kink sites, and O^{2-} ligands

The bond-valence deficiency of an edge increases with its number of kink sites, because an edge with a higher number of kink sites contains a higher ratio of stronger Lewis-bases (*e.g.*, $^{[7]}$U–φ) *versus* weaker Lewis-bases (*e.g.*, $^{[7]}$U–φ–$^{[7]}$U) (see *Calculation of bond-valence deficiency along chains of polyhedra* below). The bond-valence deficiency of an edge also increases with its number of O^{2-} ligands, because an edge with a higher number of O^{2-} ligands also has a higher ratio of stronger Lewis-bases ($^{[7]}$U–O and $^{[7]}$U–O–$^{[7]}$U) (*versus* weaker Lewis-bases, $^{[7]}$U–OH and $^{[7]}$U–OH–$^{[7]}$U). In contact with aqueous solution, the stronger Lewis-bases will either be protonated or form stronger bonds with the species in solution, which results in weakening of the corresponding U–φ bonds. Hence, edges with a higher number of kink sites or O^{2-} ligands contain a higher number of sites that can be activated during dissolution than edges with a lower number of kink sites or O^{2-} ligands.

A correlation between the growth rate of an edge and its bond-valence deficiency is not directly apparent because the edge and the cluster in solution are usually hydrated. However, a larger number of kink sites on an edge (*i.e.*, a high bond-valence deficiency) favors attachment of polyhedra because an attached polyhedron or cluster of polyhedra can share more common ligands with the corresponding polyhedra than it can on an edge with a lower number of kink sites. The negative charges of the O^{2-} ligands in a uranyl sheet closely balance the positive charge of the interstitial complex between the sheets. During crystal growth, these ligands occur on a hydrated edge, at which the ligands may be protonated differently than in the bulk structure. However, negative charges must also occur on an edge during crystal growth in order to balance the positive charge of either attached or incorporated interstitial cations. Hence, O^{2-} ligands in a bulk structure are potentially those ligands that are part of negative terminations on a protonated edge. A large number of negatively and positively charged terminations favors attachment of polyhedra or clusters of polyhedra on an edge (see below), because these terminations promote hydrogen bonding between polyhedra on an edge and the cluster in aqueous solution (*i.e.*, negatively charged terminations promote formation of activated sites during crystal growth).

The number and type of activated sites during crystal growth correlate [*via* the number of terminations (*i.e.*, the number of kink sites) and the number of negatively charged terminations] with the bond-valence deficiency of an edge in the bulk structure. The number of activated sites on an edge during dissolution or crystal growth correlates also with the difference between the pH of the solution and the pH_{pzc} of the edge (see below).

Activated sites and edges in schoepite and fourmarierite

In schoepite, $[(UO_2)_8O_2(OH)_{12}](H_2O)_{12}$, and fourmarierite, $Pb[(UO_2)_4O_3(OH)_4](H_2O)_4$, the layers have the same topology, but a different number of O and OH groups. Hence chains that terminate the [010] edge in both structures contain different numbers and types of ligands (Figs. 5a, b). At a specific pH, the [010] edge in fourmarierite must have a larger number of negatively charged terminations than the [010] edge in schoepite, because these terminations must charge-balance the incorporated or attached interstitial Pb^{2+} cations. However, at a different pH, the same chain on a [010] edge can have the same number and types of ligands in schoepite or fourmarierite. Figure 5c shows a possible model of hydration at such an edge, considering only the terminations along the edge. To activate terminations on the [010] edge of fourmarierite requires more protonation of ligands and more hydrogen bonding from the aqueous species to the ligands than on the [010] edge in schoepite. Thus the [010] edges in fourmarierite and schoepite contain different numbers and types of activated sites, even though they have identical ligands.

There are two different types of termination along the chain of polyhedra parallel to the [010] edge in schoepite and fourmarierite: U–φ and U–φ–U. Terminations of the same type have similar acid–base properties. Hence, one can assign identical hydration-models to each type of termination in schoepite and fourmarierite, *e.g.*, U–OH_2 and U–OH–U (along the chain parallel to the [010] edge). If one were to calculate the general stability of an edge based on identical models for each type of termination, one would similarly treat isostructural uranyl-sheets of different chemical composition. In other words, all equivalent edges in schoepite and fourmarierite would have similar relative stabilities. Consequently, the morphology of the (001) face should be identical on schoepite and fourmarierite crystals. However, this is not the case (see below), and therefore the different types and numbers of activated sites on edges in schoepite and fourmarierite cannot be neglected.

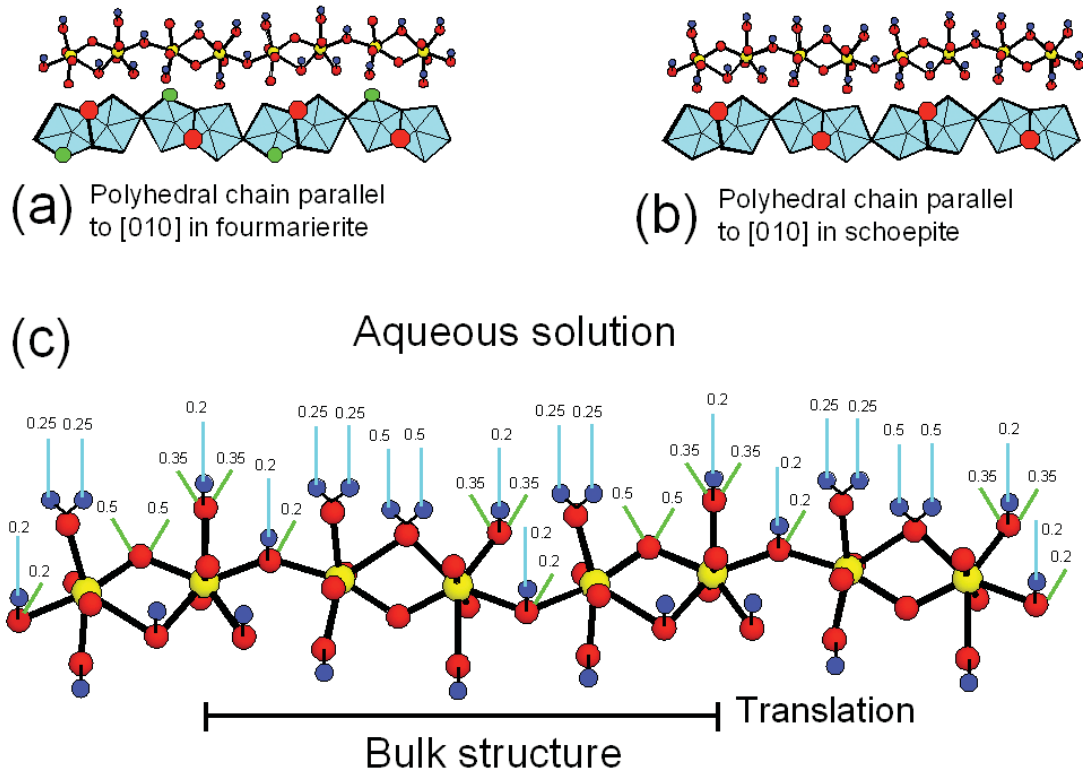

FIG. 5. (a), (b) Polyhedron and ball-and-stick representations of a chain of polyhedra parallel to [010] in fourmarierite and schoepite; in the ball-and-stick models, yellow, red and blue circles indicate U^{6+}, O^{2-} and H^{+}, respectively. In the polyhedron model, the positions of the O^{2-} equatorial ligands are indicated by green and red circles. (c) Ball-and-stick model of a possible activated edge parallel to [010]; outgoing bonds from terminations to aqueous species are indicated as blue lines, and incoming bonds accepted by the ligands of the terminations are indicated with green lines; the corresponding bond-valences (in *vu*) are given as numbers beside the lines.

pH_{pzc}, net proton-charge, inner- and outer-sphere complexes, and electric double- and triple-layers: a bond-valence perspective

The pH_{pzc} is also called the isoelectric point. Stumm (1992) defined pH_{pzc} as the point where the *total net surface-charge* is zero (this is the condition where particles do not move in an applied electric field). The total net surface-charge is the sum of (1) the permanent structural charge caused by isomorphic substitutions, (2) the net proton-charge (*i.e.*, the charge due to the binding of protons or OH-anions), (3) the charge of the inner-sphere complex, and (4) the charge of the outer-sphere complex.

The distribution of surface charge can be idealized as an electric double- or triple-layer. In the case of a double layer, the first layer is the solid surface with a localized negative surface-charge, whereas the second layer is in contact with the first layer and is a solution containing dispersed ions of positive charge (the *Gouy–Chapman diffuse model*: Stumm 1992). This model cannot be applied to surfaces of high potential because the local concentrations of counter ions near the surface becomes too large. In the Stern–Grahame triple-layer model, an additional compact layer of cations exists immediately adjacent to the mineral surface in order to balance the high charge of the surface. The ions in this layer are held tightly by "electrostatic forces" and are not free to move like the ions in the diffuse layer of the Gouy–Chapman model. Dzombak & Morel (1990) developed a surface-complexation model in which ions are attached by chemical bonding to the surface and not *via* "electrostatic effects", as assumed in the Gouy–Chapman and Stern–Grahame models. Therefore, cations of the inner-sphere complexes are treated in the surface-complexation model as part of the solid (Stumm 1992).

An inner-sphere complex and an outer-sphere complex occur if a cation or anion in the solution bonds directly or *via* (H_2O) groups to terminations on the

surface. Hence, the presence of inner-sphere and outer-sphere complexes changes the net proton-charge of the surface. If the net proton-charge is zero, the total net surface-charge is not necessarily zero. However, charge and number of inner- and outer-sphere complexes depend on many factors, such as the size and number of specific sites for complexation on the surface, and on the charge, size and activities of cations and anions in solution. We can again simplify this problem if we factor surface, inner- and outer-sphere complexes and other aqueous species into three components: (1) surface, (2) chemisorbed species, and (3) aqueous solution. To be considered part of the surface, an atom has to conform to the space-group symmetry of the crystal, with the exception of H atoms that strongly bond to O atoms at the surface. Any other atom or group of atoms chemically bonded to the surface and *not* conforming to the space-group symmetry of the crystal will not be incorporated into the structure (to any significant degree), and although chemically bonded to the surface, will have a short residence-time in this state. In some chemical systems, such chemisorbed impurities can significantly modify habit development, presumably depending on the residence lifetime of the species on the surface and the activity of that species in solution. In this way, we consider here only the change in interaction between an edge with different net proton-charges and the aqueous solution.

From a bond-valence perspective, the net proton-charge is the difference between the sums of the accepted and donated bond-valences between the termination on the surface and the species in aqueous solution. A termination that accepts bond valences is a *Lewis base*, and a termination that donates bond-valence is a *Lewis acid.* At zero net proton-charge, the strength and number of Lewis bases and Lewis acids are identical. The pH of a solution in which a surface has zero net proton-charge is called the point of zero net proton-charge, pH_{pzc} (Stumm 1992, p. 18). Depending on the intrinsic acidity-constant of the acid–base reaction, strong Lewis bases and acids occur only at low or high pH (see previous section). Hence, weaker Lewis bases and acids occur mainly on a surface at the pH_{pzc}. This approach emphasizes that at the pH_{pzc}, the bond-valence transfer between Lewis bases and acids on the surface and the aqueous solution is at a minimum.

An example: bond-valence transfer along a chain of polyhedra in schoepite and fourmarierite

Consider a chain of polyhedra parallel to the [010] edge in schoepite or fourmarierite (Fig. 5c). There are eight terminations ($4 \times$ [7]U–φ and $4 \times$ [7]U–φ–[7]U) per repeat length of the chain, and these interact with the aqueous solution. Figure 5c shows a hydration model for this chain, in which the incoming and outgoing bonds are shown in green and blue, respectively. In the repeat period of the chain, there are one U–O–U, one U–OH_2–U, two U–OH, two U–OH_2 and two U–OH–U terminations. In order to simplify the bond-valence calculations involving the incoming and outgoing bonds, we assign an average bond-valence of 0.50 *vu* to a [7]U–φ bond. An atom of oxygen of a [7]U–OH_2 group receives 0.50 *vu* from the [7]U–O bond and requires an additional 2×0.75 *vu* from the two O–H bonds in order to satisfy its bond-valence requirements. The two H-atoms require 0.25 *vu* from hydrogen bonds to an aqueous species in order to satisfy their own bond-valence requirements. Hence, any [7]U–OH_2 group donates two hydrogen bonds, each with a bond-valence of 0.25 *vu*, to the aqueous species.

An atom of oxygen of a [7]U–OH group receives 0.50 *vu* from the [7]U–O bond and requires an additional 1.50 *vu*. The O–H bond has a bond valence of 0.80 *vu*, and the oxygen atom thus requires an additional 0.70 *vu* from bonds from the aqueous species (Fig. 5c). In the same way, an atom of oxygen of an U–OH–U group receives 2×0.50 *vu* from two [7]U–O bonds and 0.80 *vu* from the hydrogen atom of the OH-group, and requires an additional 0.20 *vu* from a bond (or bonds) from an aqueous species. Hence, an atom of oxygen of a [7]U–O–[7]U group requires an additional 1.0 *vu* from bonds involving the aqueous species. The oxygen atom of a [7]U–OH_2–[7]U group accepts 2×0.50 *vu* from two [7]U–O bonds and requires an additional 2×0.50 *vu* from two O–H bonds; therefore, the [7]U–OH_2 group donates two hydrogen bonds with a bond-valence of 0.50 *vu*. The corresponding acid–base equilibria between the different Lewis bases and acids are listed in Table 1. The *pKa* values indicate that strong Lewis bases (such as [7]U–O–[7]U and [7]U–OH_2–[7]U) occur only at high and low pH, respectively. Thus the number of strong Lewis bases and acids on the [010] edge is very small in weak acidic, weak basic and neutral solutions.

We can now calculate aggregate bond-valences involving the outgoing and incoming bonds. There are $2 \times 0.20 + 4 \times 0.25 + 2 \times 0.20 + 2 \times 0.50 = 2.8$ *vu* donated from the terminations to the aqueous species, and there are $4 \times 0.35 + 2 \times 0.20 + 2 \times 0.50 = 2.80$ *vu* (Fig. 5) accepted from the terminations. The overall transfer of bond valence from or to the chain is thus $2.8 + 2.8 = 5.6$ *vu*. Because the accepted and donated bond-valences are equal, the chain is formally neutral. This is not surprising, as the number of the formally negatively charged terminations U–O–U (–1.0 *vu*) and U–OH (–0.50 *vu*) is equal to the number of formally positively charged terminations U–OH_2–U (+1.0 *vu*) and U–OH_2 (+0.5 *vu*), respectively.

If the pH of the solution is the same as the pH_{pzc}, there is not only an equal number of positively and negatively charged anion species, but there is also a minimum number of strong Lewis acids or bases such as U–O–U and U–OH_2–U at a given ionic strength of the solution. If the number of these terminations is infinitely small, the bond-valence transfer to or from the chain minimizes at 1.8 *vu*. If the pH differs from the pH_{pzc},

the Lewis acidities or basicities of the terminations vary sympathetically in both number and strength.

Consider an increase in the number of U–OH and U–OH_2 species. For four U–OH_2 and four U–OH–U terminations, there are $4 \times 0.20 + 8 \times 0.25 = 2.8$ *vu* donated by the terminations to the aqueous species, and there are $4 \times 0.20 = 0.80$ *vu* accepted by the terminations. The formal charge of this chain per repeat distance is $2.8 - 0.8 = 2^+$. For four U–OH terminations and four U–OH–U terminations, the terminations accept $8 \times 0.35 + 4 \times 0.20 = 3.6$ *vu* and donate $4 \times 0.2 + 4 \times 0.20 = 1.6$ *vu*; the *total* transfer of bond valence is $3.6 + 1.6 = 5.2$ *vu*, and the *net* transfer of bond valence is $1.6 - 3.6 = 2.0$ *vu*. These examples illustrate the fact that an increase in the number of U–OH or U–OH_2 terminations increases the total bond-valence transfer to and from the terminations, but not necessarily the net bond-valence transfer. The configuration of four U–OH_2 and four U–OH–U terminations results in a total bond-valence transfer of $2.8 + 0.80 = 3.6$ *vu*, which is equal to the minimum transfer at neutral charge: $1.8 + 1.8 = 3.6$ *vu*. The minimum total bond-valence transfer thus does not automatically occur at an edge with zero charge. However, an increase in the number of U–OH_2 terminations is normally the result of a decrease in pH, which also produces a higher ratio of U–OH_2–U to U–O–U terminations. A higher number of U–OH_2–U terminations increases the total bond-valence transfer, which will be higher than the minimum transfer at neutral charge.

From this discussion, we can define the pH_{pzc} of a surface from a bond-valence perspective (not considering inner- or outer-sphere complexes): *At the pH_{pzc} of a surface, there is a minimum in the number of highly charged terminations (i.e., strong Lewis acids and Lewis bases) on the surface, which results in low bond-valence transfer between surface acceptors and donors and the aqueous species.*

A higher number of strong bonds between terminations and aqueous species enhances attachment and detachment of polyhedra or groups of polyhedra, and growth or dissolution rates should correlate with the type and number of activated sites.

pH_{pzc}: faces

A surface may be positive, negative or neutral. The bond-valence deficiency at a face is a measure of the bond valence required to achieve electroneutrality at that face. If there is a low bond-valence deficiency at a face and the pH of the solution is identical to the pH_{pzc}, there is a low interaction between the face and the solution. This results in formation of only a small number of activated sites, and hence the dissolution rate perpendicular to the face is small.

Two examples: calculation of the pH_{pzc} of the (001) face of schoepite and dehydrated schoepite

Schoepite, $[(UO_2)_8O_2(OH)_{12}](H_2O)_{12}$, has a prominent basal (001) face that dominates the morphology of its crystals. The pH_{pzc} occurs where the average composition of the surface is equal to the composition of the structural unit, $[(UO_2)_8O_2(OH)_{12}]$. On the basis of the *pKa* values in equations [1] to [3], the $^{[7]}$U–φ–$^{[7]}$U termination occurs over a wide range of pH as $^{[7]}$U–OH–$^{[7]}$U, and is therefore not involved in acid–base reactions close to the pH_{pzc}. There are twelve $^{[7]}$U–φ–2$^{[7]}$U terminations in the asymmetric unit; two of them occur as $^{[7]}$U–O–2$^{[7]}$U, and ten of them as $^{[7]}$U–OH–2$^{[7]}$U. In order to have an average composition of the surface of $[(UO_2)_8O_2(OH)_{12}]$, there must be five times more $^{[7]}$U–OH–2$^{[7]}$U terminations than the $^{[7]}$U–O–2$^{[7]}$U termination. The pH_{pzc} can be calculated *via* the Henderson–Hasselbach equation (Atkins 1996) on the basis of the *pKa* value and the ratio of the terminations in the asymmetric unit:

$$pH_{pzc} = pH = pKa - \log [acid]/[base]$$
$$= 7.72 - \log [5]/[1] = 7.02 \quad (11).$$

In the case of dehydrated schoepite, the composition of the surface at pH_{pzc} must be identical to the composition of the structural unit, $[(UO_2)O_{0.2}(OH)_{1.6}]^0$. This is the case, as there are eight times more U–(OH)–2U terminations than U–O–2U terminations. On the basis of the experimentally determined pKa value of 7.0 (see above), the pH_{pzc} of dehydrated schoepite is therefore

$$ph_{pzc} = pH = pKa - \log [8]/[1]$$
$$= 7.0(2) - 0.9 = 6.1 \quad (12).$$

pH_{pzc}: edges

Because of the prominent basal faces in uranyl minerals, the formal charges at the different edges may contribute only a small amount to the overall surface-charge. However, the individual pH_{pzc} of an (activated) edge and the pH of the solution will control crystal growth and dissolution at this specific edge. Thus accurate prediction about the occurrence of edges can only be made if one knows their pH_{pzc}.

Example: calculation of the pH_{pzc} for edges on the (001) face of schoepite

The following anion-terminations occur on the edges of the (001) face of schoepite: $^{[7]}$U–O, $^{[7]}$U–OH, $^{[7]}$U–OH_2, $^{[7]}$U–O–$^{[7]}$U, $^{[7]}$U–OH–$^{[7]}$U, $^{[7]}$U–O–2$^{[7]}$U and $^{[7]}$U–OH–2$^{[7]}$U. The $^{[7]}$U–O, $^{[7]}$U–OH, $^{[7]}$U–O–$^{[7]}$U and $^{[7]}$U–O–2$^{[7]}$U terminations have formal negative charges of ~1.5, 0.5, 1 and 0.50, respectively. They all have a bond-valence deficiency and interact with the solution by accepting bond-valence *via* protonation or hydrogen

bonding. The $^{[7]}U–OH_2$, $^{[7]}U–OH_2–^{[7]}U$ and $^{[7]}U–OH–2^{[7]}U$ terminations have formal positive charges of ~0.5, 1 and 0.5, and interact with the solution by donating hydrogen bonds to aqueous species. The $^{[7]}U–OH–^{[7]}U$ anion-termination has a formal charge of zero and may both accept and donate one hydrogen bond. The charge on an edge is zero if there is an equal number of $^{[7]}U–OH_2$ and $^{[7]}U–OH$ terminations, $^{[7]}U–OH_2–^{[7]}U$ and $^{[7]}U–O–^{[7]}U$ terminations, and $^{[7]}U–O–2^{7]}U$ and $^{[7]}U–OH–2^{[7]}U$ terminations. Because $^{[7]}U–\varphi$ and $^{[7]}U–\varphi–^{[7]}U$ are the dominant terminations on the edges of schoepite, the pH_{pzc} of the edges is defined primarily by the following acid–base reactions:

$$^{[7]}U–O–^{[7]}U + H^+ \leftrightarrow {}^{[7]}U–OH–^{[7]}U, \quad pKa = 13.07 \qquad [5]$$

$$^{[7]}U–OH–^{[7]}U + H^+ \leftrightarrow {}^{[7]}U–OH_2–^{[7]}U, \quad pKa = 1.2 \qquad [6]$$

$$^{[7]}U–OH + H^+ \leftrightarrow {}^{[7]}U–OH_2, \quad pKa = 6.53 \qquad [7]$$

There are equal numbers of $^{[7]}U–OH_2–^{[7]}U$ and $^{[7]}U–O–^{[7]}U$ terminations at pH = (13.07 + 1.2) / 2 = 7.135, and an equal number of $^{[7]}U–OH$ and $^{[7]}U–OH_2$ terminations at pH = 6.534. Thus, every edge on the (001) face of schoepite has its pH_{pzc} at ~6.5 < pH < ~7.1. If the pH of the solution is in this range, there is the lowest interaction between the activated sites on an edge and the species in aqueous solution. [Note that as indicated above, the MUSIC equation in this form might not fit *all* uranyl-oxide minerals, and the calculated values of *pKa* should be seen as approximations rather than exact values.] This example shows that the pH_{pzc} of an edge cannot be used to predict its occurrence on a basal face. However, pH_{pzc} enables us to predict the *change* in morphology with a change in pH from the range in pH_{pzc} of the edges.

Change in morphology with change in pH

The change in morphology with change in pH depends strongly on the degree of supersaturation in the aqueous fluid. At high supersaturation, a large number of aqueous species will simultaneously attach to the surface, resulting in rough surfaces with fast growth-rates. In this case, the number and type of protonated anion-terminations will not be relevant for a slow-growth process in which the attachment of aqueous species produce smooth surfaces with a low number of kink sites. Hence, the following discussion on the effect of pH on the morphology is restricted to solutions at low supersaturation.

Figure 6 shows how the occurrence of an edge may vary with change in pH. Let us consider the edge with the lowest bond-valence deficiency of all possible edges. If the edge interacts with a solution of pH close to its pH_{pzc}, there is a weak interaction between the anion terminations and the aqueous species. The corresponding edge would contain only a small number of activated sites (see above), the dissolution or crystallization rate would be small, and the edge would survive on the final morphology of the basal face. If the pH of the solution differs from the pH_{pzc} by an amount ΔpH, there is a greater interaction between the terminations and the aqueous species. The number of activated sites increases with increasing ΔpH. However, the corresponding edge would still occur on the final morphology of the basal face, and depending on the bond-valence deficiency of the other edges, it might even dominate the morphology of the basal face (Fig. 6).

The explanation of this phenomenon can be found if we consider next an edge with an average bond-valence deficiency (*i.e.*, this edge has a higher bond-valence deficiency than the edge considered previously). At a pH close to its pH_{pzc} value, its anion terminations would interact slightly more with the solution than those of the previously considered edge. The resulting activated edge would therefore contain a higher number of activated sites than the previous activated edge. However, if the interaction between the second edge and a solution with a pH = pH_{pzc} of the second edge is still small, the corresponding dissolution or crystallization rates would be similar to the rates of dissolution or crystallization of the previous edge, and the edge would occur on the final basal face. The occurrence of those edges is therefore strongly controlled by the relation between dissolution or crystallization kinetics and ΔpH.

If ΔpH increases dramatically, the already higher number of activated sites will increase even more, and the morphology will change (Fig. 6). In this case, the higher rates of dissolution or crystallization (in comparison to the previous edge) presumably result in disappearance of the edge during growth or dissolution. Hence at higher ΔpH, the final morphology of a basal face is defined by the edges with the lowest bond-valence deficiency.

Finally, let us consider an edge with the highest bond-valence deficiency. The interaction of its terminations with an aqueous solution of a specific ΔpH will be the highest of all previous edges; *i.e.*, there is a high probability that the corresponding rates of dissolution or crystallization may be so high that the edge will disappear during these processes. Under normal circumstances, edges with the highest bond-valence deficiency should therefore never occur on the final morphology of the basal faces.

Similar considerations apply to the supersaturation parameter, β. At equilibrium, the saturation of a solution is unity ($\beta = 1$), and there is a minimum in the interaction between activated sites and species in aqueous solution. Where supersaturation increases or decreases by $\Delta\beta$, the interaction between aqueous solution and edge increases. Hence at high $\Delta\beta$, one would expect edges with the lowest bond-valence deficiency, whereas

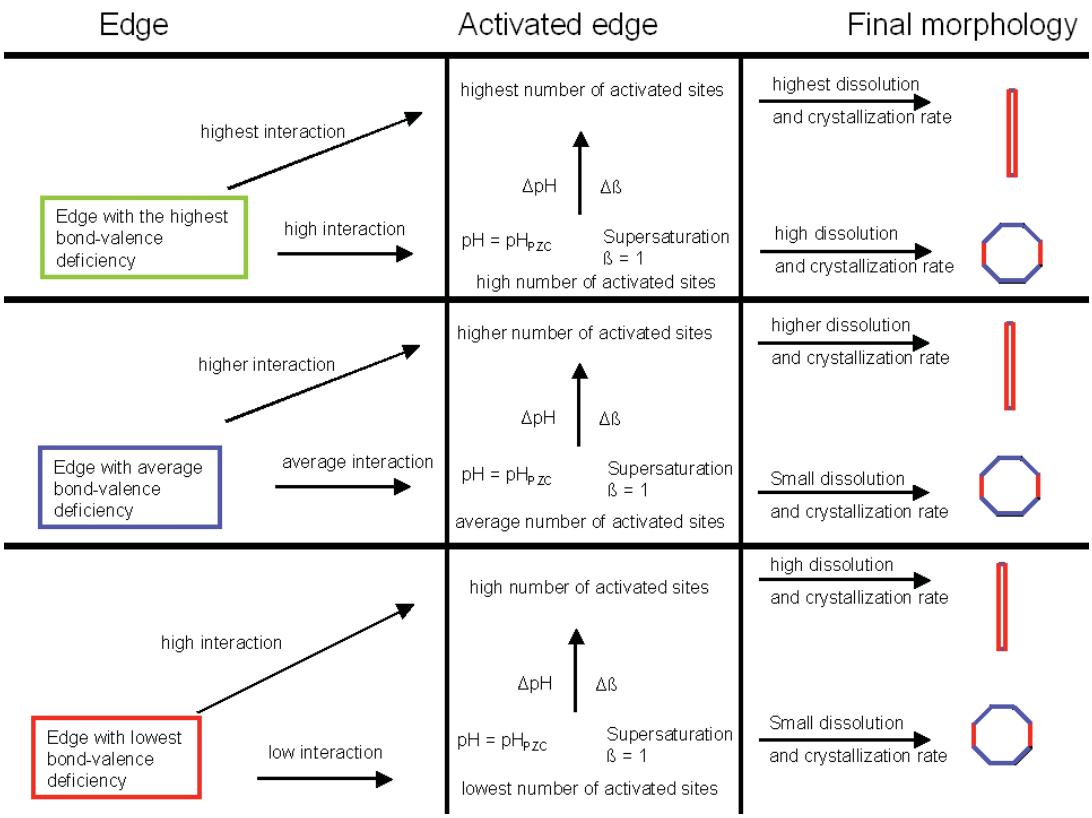

FIG. 6. The left column lists the possible types of edges: edges with lowest, average and highest bond-valence deficiencies are indicated in red, blue and green, respectively. The central column schematically indicates the increase in activated sites with (a) the initial bond-valence deficiency of the edge, (b) the difference between the pH of the solution and the pH_{pzc} of the edge (indicated as ΔpH), and (c) the difference between the supersaturation, β, of a solution and the supersaturation at equilibrium, with β = 1 (indicated as Δβ). The increase in ΔpH and Δβ is indicated by an arrow. The right column lists the corresponding rates of dissolution and crystal growth, and the final morphologies of a theoretical (001) face. The colors of the edges indicate the corresponding bond-valence deficiencies of the edges.

at low Δβ, one would expect edges of low and average bond-valence deficiency.

Change in morphology with stacking sequences of layers

An edge terminates one layer and can be characterized by a chain of polyhedra in the layer. A face crossing the layers terminates more than one layer, and this surface is characterized by chains of polyhedra that terminate the different layers. If adjacent layers are shifted relative to each other, the face can be terminated by different types of chains. Figure 7a shows sequence of layers with or without a shift between the layers. There are interstitial cations, (H_2O) or (OH) groups between each layer.

Arrangements (1) to (3) (Fig. 7) show three layers that are terminated by one type of chain of polyhedra. The chain indicated by a yellow rectangle has a lower bond-valence deficiency than the chains indicated by green rectangles, and hence edges in arrangements (1) and (3) are more stable than edges in arrangement (2). In arrangements (4) to (6), the layers contain the same type of chains of polyhedra. However, the central layer is shifted by one polyhedron relative to the adjacent layers. In this case, two chains of high bond-valence deficiency and one chain of low bond-valence deficiency terminate the edges in arrangement (4). Edges on a face that are terminated by chains of high and low bond-valence deficiencies have different growth and dissolution rates. Hence, in Figure 7a, the upper and lower layers grow faster than the central layer. This growth mechanism results in arrangement (5), in which only chains of lower bond-valence deficiency terminate an edge. Thus, edges in arrangement (5) are more stable than edges in arrangement (4). Arrangement (5) con-

tains one major kink-site with interstitial complexes above and below. The rates of growth and dissolution at this kink-site are therefore not only characterized by the bond-valence deficiency of the chain; they are also controlled by the acidity of the interstitial complex. This is in contrast to arrangement (1), in which the rates of growth and dissolution are determined only by the bond-valence deficiency of the chains. Thus, edges in arrangement (5) are less stable than edges in arrangement (1).

Figure 7b shows the same type of arrangements as in Figure 7a, but with chains of average and high bond-valence deficiency (indicated by pink and green rectangles, respectively). The stabilities of edges in the corresponding arrangements are the same, *i.e.*, edges in arrangement (7) have a higher stability than edges in arrangement (11). The difference in bond-valence deficiency can now be used to compare the stability of edges that have a similar shift between their layers. Edges in arrangement (1) have a lower bond-valence deficiency than edges in arrangement (7), and therefore, the former are more stable and have lower rates of dissolution and growth than the latter (Fig. 7c). In the same way, edges in arrangement (5) are more stable than edges in arrangement (11), and therefore the former also have lower rates of dissolution and growth than the latter (Fig. 7c).

The kink sites of arrangements (5) and (11) are characterized by the acidity of the adjacent interstitial com-

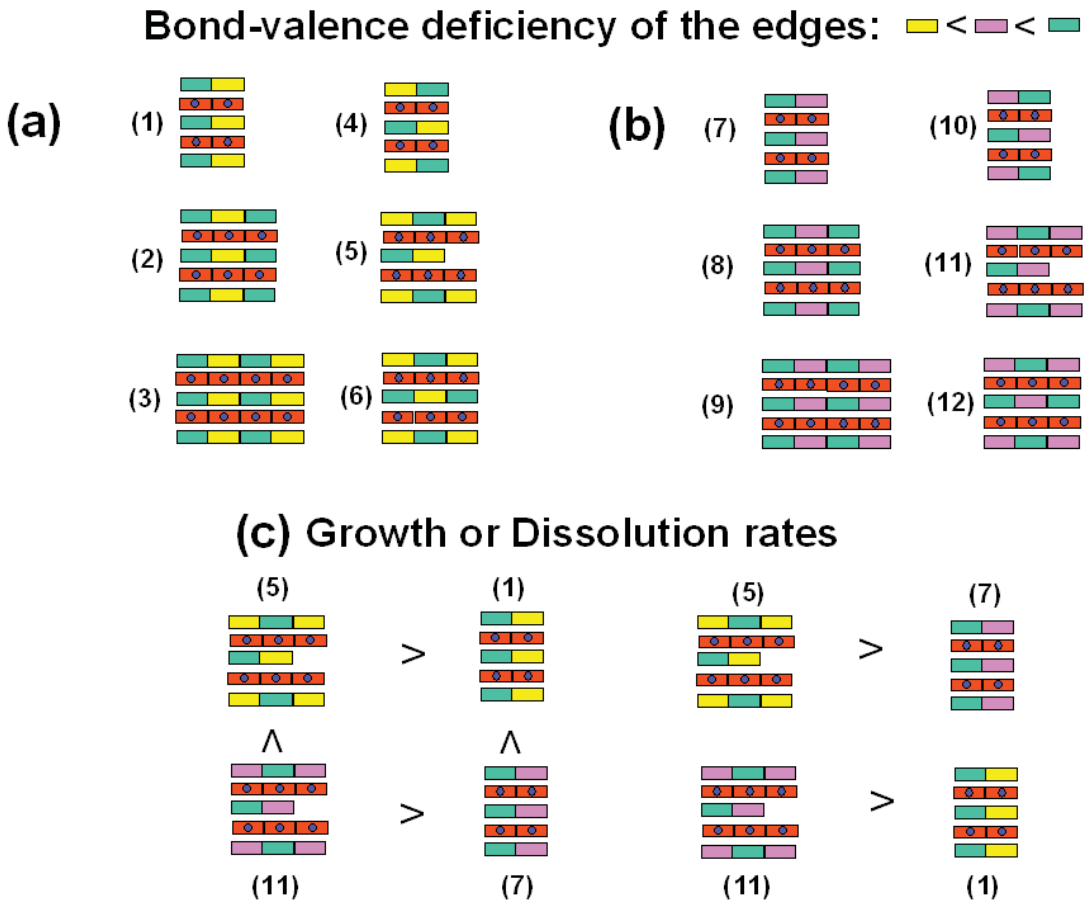

FIG. 7. Schematic representation of different sequences in the stacking of layers, with chains of different bond-valence deficiencies. (a) Chains are indicated as yellow (low bond-valence deficiency) and green (high bond-valence deficiency) rectangles, and interstitial complexes are indicated with red rectangles and blue circles. Arrangements (1) to (6) display growth sequences of edges with identical chains but with different shifts between the layers. (b) Arrangements (7) to (12) are identical to arrangements (1) to (6) owing to the shift between the layers, but have chains of average and low bond-valence deficiency (indicated as pink and green rectangles). (c) Growth and dissolution rates among the different arrangements (for details, see text).

plexes and by the bond-valence deficiency of the chain of polyhedra. Hence, there are three components at these kink sites that interact with the aqueous species. The corresponding edges thus interact more extensively with the aqueous solution than edges in arrangements (1) and (3). Hence, we predict that edges in arrangements (5) and (11) have lower stability than edges in arrangements (1) and (7).

Change in morphology with change in arrangement of interstitial complexes

A change in morphology of the basal face with change in arrangement of the interstitial complex can be observed in minerals with identical structural units, identical shifts between the layers, but different arrangements of their interstitial complexes. This is the case for becquerelite, $^{[7]}Ca(H_2O)_4[(UO_2)_3O_2(OH)_3]_2(H_2O)_4$, and billietite, $^{[10]}Ba(H_2O)_4[(UO_2)_3O_2(OH)_3]_2\ (H_2O)_3$. Figures 8a and 8b show the arrangements of the interstitial cations Ca and Ba in becquerelite and billietite, respectively. The interstitial Ca atoms in becquerelite are arranged in rows parallel to [010], whereas the interstitial Ba atoms in billietite are arranged in rows parallel to [100]. Evaluation of the bond-valence deficiencies (taking into account the shift between the layers in each structure) indicates that [100] and [110] are the most stable edges, whereas edges such as [100], [210], [130] and [310] are less stable. Hence, we predict that the edges [100] and [110] invariably occur, independent of pH and saturation, whereas all other edges occur only close to the pH_{pzc} and at saturation.

Becquerelite and billietite crystals strongly resemble each other in color and form. The edges [100] and [110] invariably occur on their (001) face, in good agreement with our predictions. Only becquerelite crystals are reported as elongate parallel to [010], whereas billietite crystals can be elongate parallel to [100] [Figs. 8a and 8b; Perloff (1998); http://www.trinityminerals.com/sm2001/uranium.shtml]. This implies that the occurrence of edges and their dominance on the final morphology may be also controlled by the arrangement of the interstitial complexes. We may summarize the above discussion as follows: (a) If we consider only the struc-

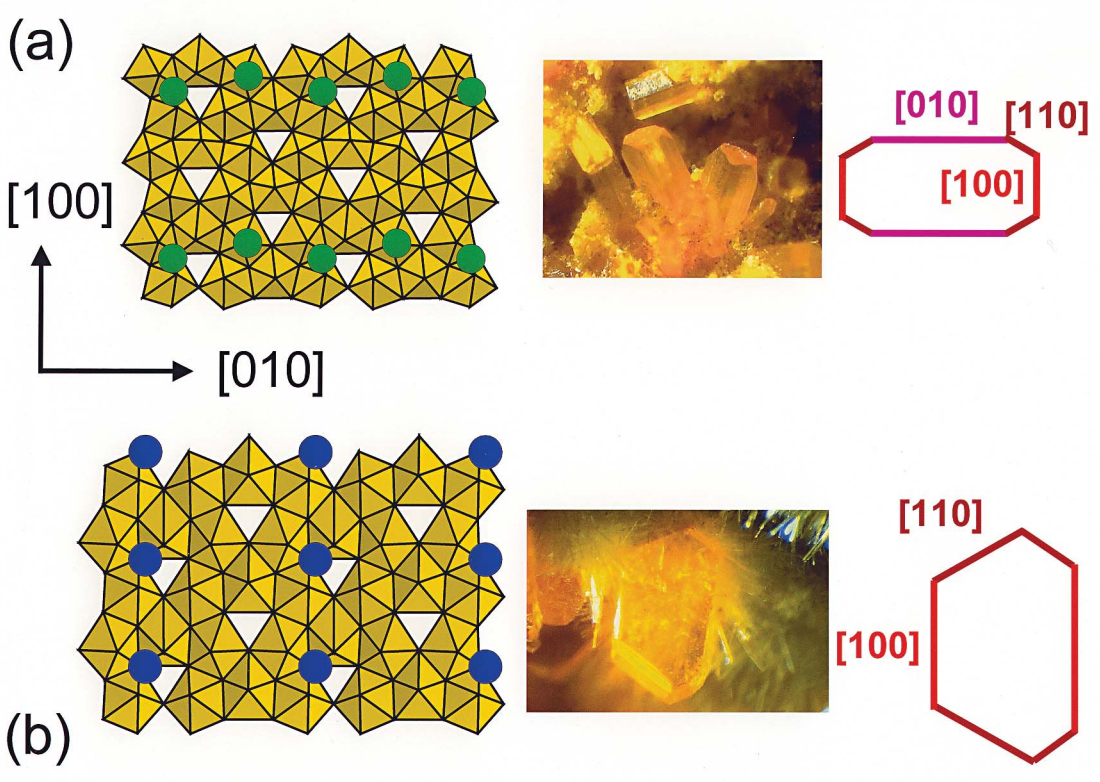

FIG. 8. Left: polyhedron illustrations of layers in (a) becquerelite, and (b) billietite, showing the positions of the interstitial Ca (green circles) and Ba (blue circles). Right: examples of the corresponding (001) face morphologies on becquerelite and billietite crystals (for details, see text).

tural information of the uranyl sheets, we can predict the occurrence (or non-occurrence) of edges with the lowest and highest bond-valence deficiencies. (b) If we consider also the pH_{pzc}, pH, degree of saturation and the arrangement of the interstitial complex, we can predict the occurrence of edges with average bond-valence deficiency.

Calculation of bond-valence deficiency along chains of polyhedra

In order to predict the occurrence of different edges, we must consider the different types of linear periodic chains of polyhedra parallel to an edge. Figure 9 shows linear periodic chains of polyhedra parallel to [100] in schoepite. Depending on whether one considers the surface on the right or left side of the figure, one can construct (linear periodic) chains of polyhedra with different types of terminations (Figs. 9a, c). Terminations of linear periodic chains that terminate the layer to the right or left side are called *right terminations* or *left terminations*, respectively.

The linear periodic chain of polyhedra parallel to [100] has a repeat distance of 14.377 Å. Let us designate the left termination of this chain as *a1*: there are two $^{[7]}$U–OH terminations and four $^{[7]}$U–OH–$^{[7]}$U terminations (Fig. 9a). The average bond-valence of $^{[7]}U^{6+}$–O in schoepite is 0.47 *vu*, and the average O–H bond-valence is 0.80 *vu* (Brown 1981). The oxygen atoms of the two [1]-coordinated and the four [2]-coordinated (OH) groups receive $(2 \times 1 \times 0.47 + 2 \times 0.8) = 2.54$ *vu*, and $(4 \times 2 \times 0.47 + 4 \times 0.8) = 6.96$ *vu*, respectively. The resulting bond-valence deficiency at the oxygen atoms in the chain is the difference between their formal valence and their incident bond-valence sum. For example, the oxygen atoms of the two [1]-coordinated (OH) groups in the repeat unit of the chain have a formal charge of 4^-, and they accept 2×0.47 *vu* from equatorial U–O bonds and 2×0.80 *vu* from O–H bonds. The sum of the incident bond-valence is 2.54 *vu*, result-

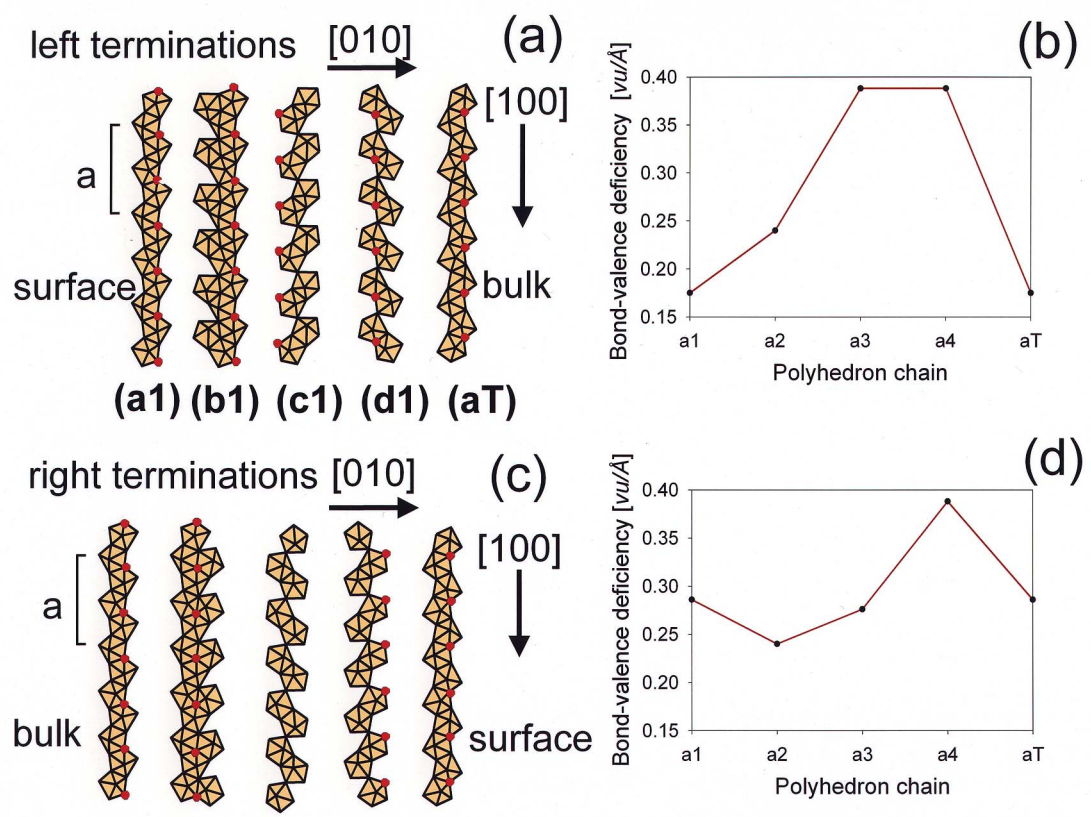

FIG. 9. (a) The left form of chain termination for different chains parallel to the [100] edge in the uranyl sheet of schoepite; the positions of the O^{2-} anions are indicated by red circles. At each chain, the bulk structure continues to the left, and the surface occurs at the right side. (b) The calculated bond-valence deficiency per unit length (*vu* / Å) of anion terminations on chain terminations of the left form. (c) The right form of chain terminations for different chains parallel to the [100] edge. (d) The corresponding bond-valence deficiency per unit length of the anion terminations on chain terminations of the right form.

ing in an aggregate bond-valence deficiency of 4 – 2.54 = 1.46 *vu*. The bond-valence deficiency of the four [2]-coordinated oxygen atoms is 1.04 *vu*. The bond-valence deficiency of the oxygen atoms in the repeat distance of the chain of polyhedra is 1.46 + 1.04 = 2.50 *vu*, and normalized to the length of the chain: 2.50 / 14.337 = 0.1744 *vu* / Å.

The bond-valence deficiency of such a chain depends on the type and number of anion terminations. A high bond-valence deficiency occurs where the chain contains a high number of negatively charged terminations, such as U–OH (–0.5), U–O–U (–1.0) or U–O (–1.5 *vu*), and a low bond-valence deficiency occurs if the chain contains a high number of the formally neutral U–OH–U terminations. Here, the number of kink sites along the chain controls the number of U–φ and U–φ–U terminations.

Summary

(1) The bond valence of an anion termination on a terminating chain of polyhedra correlates with the intrinsic acidity-constant, *pKa*, and with the free energy, ΔG_{at}, of the corresponding acid–base reaction.

(2) The bond-valence deficiency of a linear periodic chain of polyhedra parallel to an edge correlates with the type and number of activated sites on an edge.

(3) Processes of crystal growth and dissolution on an edge are catalyzed by the activated sites and increase with their number and the strength of the bonds between the corresponding anion terminations and the aqueous species.

(4) The interaction between activated sites and aqueous species is minimized where the pH of the solution is at the pH_{pzc} of the edge and where the solution is close to saturation with respect to the mineral.

(5) Interaction of an edge with the aqueous solution during crystal growth and dissolution depends also on the shift between the layers and the arrangement of the interstitial complexes between the layers.

(6) One can use the latter parameters and the bond-valence deficiency of a polyhedron to predict the occurrence of edges on the basal face of uranyl-sheet minerals.

Acknowledgements

We thank referees Mike Hochella and Cornelis Woensdregt and Editor Bob Martin for their comments, which added considerably to the clarity of this paper. MS and AP thank the Deutsche Forschungsgemeinschaft for an Emmy Noether Fellowship and grant P153/10-1, respectively. FCH was supported by a Canada Research Chair in Crystallography and Mineralogy and by a Discovery Grant from the Natural Sciences and Engineering Research Council of Canada.

References

Atkins, P.W. (1996): *Physikalische Chemie* (zweite Auflage). VCH Verlagsgesellschaft, Weinheim, Germany.

Bargar, J.R., Brown, G.E., Jr., & Parks, G.A. (1997a): Surface complexation of Pb(II) at oxide–water interfaces. 1. XAFS and bond-valence determination of mononuclear and polynuclear Pb(II) sorption products on aluminum oxides. *Geochim. Cosmochim. Acta* **61**, 2617-2637.

_____, _____ & _____ (1997b): Surface complexation of Pb(II) at oxide–water interfaces. 2. XAFS and bond-valence determination of mononuclear and polynuclear Pb(II) sorption products and surface functional groups on iron oxides. *Geochim. Cosmochim. Acta* **61**, 2639-2652.

_____, Towle, S.N., Brown, G.E. & Parks, G.A. (1997c): XAFS and bond-valence determination of the structures and compositions of surface functional groups and Pb(II) and Co(II) sorption products on single-crystal α-Al_2O_3. *J. Colloid Interface Sci.* **185**, 473-492.

Bickmore, B.R., Rosso, K.M., Nagy, K.L., Cygan, R.T. & Tadanier, C.J. (2003): Ab initio determination of edge surface structures for dioctahedral 2:1 phyllosilicate: implications for acid–base reactivity. *Clays Clay Minerals* **51**, 359-371.

Brown, G.E., Jr., & Parks, G.A. (2001): Sorption of trace elements on mineral surfaces: modern perspectives from spectroscopic studies, and comments on sorption in the marine environment. *Int. Geol. Rev.* **43**, 963-1073.

Brown, I.D. (1981): The bond-valence method: an empirical approach to chemical structure and bonding. *In* Structure and Bonding in Crystals II (M. O'Keeffe & A. Navrotsky, eds.). Academic Press, New York, N.Y. (1-30).

_____ & Altermatt, D. (1985): Bond-valence parameters obtained from a systematic analysis of the inorganic crystal structure database. *Acta Crystallogr.* **B41**, 244-247.

_____ & Shannon, R.D. (1973): Empirical bond-strength – bond-length curves for oxides. *Acta Crystallogr.* **A29**, 266-282.

Burns, P.C. (1999): The crystal chemistry of uranium. *In* Uranium: Mineralogy, Geochemistry and the Environment (P.C. Burns & R. Finch, eds.). *Rev. Mineral.* **38**, 23-90.

Dzombak, D.A. & Morel, F.M.M. (1990): *Surface Complexation Modeling: Hydrous Ferric Oxide*. John Wiley & Sons, New York, N.Y.

Faure, G. (1998): *Principles and Applications of Geochemistry* (2nd ed.). Prentice Hall, Upper Saddle River, New Jersey.

Finch, R.J., Cooper, M.A., Hawthorne, F.C. & Ewing, R.C. (1996): The crystal structure of schoepite, $[(UO_2)_8O_2(OH)_{12}](H_2O)_{12}$. *Can. Mineral.* **34**, 1071-1088.

HARTMAN, P. & PERDOK, W.G. (1955a): On the relations between structure and morphology of crystals I. *Acta Crystallogr.* **8**, 49-52.

_____ & _____ (1955b): On the relations between structure and morphology of crystals II. *Acta Crystallogr.* **8**, 521-524.

_____ & _____ (1955c): On the relations between structure and morphology of crystals III. *Acta Crystallogr.* **8**, 525-529.

HAWTHORNE, F.C. (1985): Towards a structural classification of minerals: the $^{vi}M^{iv}T_2\varphi_n$ minerals. *Am. Mineral.* **70**, 455-473.

_____ (1986): Structural hierarchy in $^{VI}M_x^{III}T_y\varphi_z$ minerals. *Can. Mineral.* **24**, 625-642.

_____ (1990): Structural hierarchy in $M^6T^4\varphi_n$ minerals. *Z. Kristallogr.* **192**, 1-52.

_____ (1994) Structural aspects of oxides and oxysalt crystals. *Acta. Crystallogr.* **B50**, 481-510.

_____ (1997): Structural aspects of oxide and oxysalt minerals. *In* Modular Aspects of Minerals (S. Merlino, ed.). *Eur. Mineral. Union, Notes in Mineralogy* **1**, 373-429.

HIEMSTRA, T., VENEMA, P. & VAN RIEMSDIJK, W.H. (1996): Intrinsic proton affinity of reactive surface groups of metal (hydr)oxides: the bond valence principle. *J. Colloid Interface Sci.* **184**, 680-692.

LEWIS, G.N. (1916): The atom and the molecule. *J. Am. Chem. Soc.* **38**, 762-785.

MOLL, H., REICH, T. & SZABÓ, Z. (2000): The hydrolysis of dioxouranium (VI) investigated using EXAFS and ^{17}O-NMR. *Radiochim. Acta* **88**, 411-415.

PERLOFF, L. (1998): *The Photo-Atlas of Minerals* (A.R. Kampf & G. Gerhold, eds.). The Gem and Mineral Council, Los Angeles County Museum of Natural History, Los Angeles, California.

RUFE, E. & HOCHELLA, M., JR. (1999): Quantitative assessment of reactive surface area of phlogopite dissolution during acid dissolution. *Science* **285**, 874-876.

SCHINDLER, M. & HAWTHORNE, F.C. (2001a): A bond-valence approach to the structure, chemistry and paragenesis of hydroxy-hydrated oxysalt minerals. I. Theory. *Can. Mineral.* **39**, 1225-1242.

_____ & _____ (2001b): A bond-valence approach to the structure, chemistry and paragenesis of hydroxy-hydrated oxysalt minerals. II. Crystal structure and chemical composition of borate minerals. *Can. Mineral.* **39**, 1243-1256.

_____ & _____ (2001c): A bond-valence approach to the structure, chemistry and paragenesis of hydroxy-hydrated oxysalt minerals. III. Paragenesis of borate minerals. *Can. Mineral.* **39**, 1257-1274.

_____ & _____ (2004): A bond-valence approach to the uranyl-oxide hydroxy-hydrate minerals: chemical composition and occurrence. *Can. Mineral.* **42**, 1601-1627.

_____, _____ & BAUR, W.H. (2000): A crystal-chemical approach to the composition and occurrence of vanadium minerals. *Can. Mineral.* **38**, 1443-1456.

STUMM, W. (1992): *Chemistry of the Solid–Water Interface*. John Wiley & Sons, New York, N.Y. (428).

SUNAGAWA, I. (1987): Morphology of minerals. *In* Morphology of Crystals (I. Sunagawa, ed.). Terrapub, Tokyo, Japan (509-587).

Received August 12, 2003, revised manuscript accepted September 7, 2004.